FUSE

Fungal Systematics and Evolution

VOLUME 17
JUNE 2026
PAGES 184–220

Diversity of fungal species belonging to *Hypocreales* and recovered in a cultural heritage environment, with an emphasis on Paleolithic decorated caves

J. Leplat[1,2]*, A. François[1,2], F. Bousta[1,2]

[1]Centre de Recherche sur la Conservation (CRC, USR 3224), Museum national d'Histoire naturelle, CNRS, Ministère de la Culture, 36 rue Geoffroy-Saint-Hilaire, 75005 Paris, France
[2]Laboratoire de Recherche des Monuments Historiques (LRMH), Ministère de la Culture, 29 rue de Paris, 77420 Champs-sur-Marne, France

*Corresponding author: johann.leplat@culture.gouv.fr

Keywords:
arthropods,
Cordycipitaceae,
cultural heritage,
fungal phylogeny,
new taxa

Abstract: Fungi are a major concern in terms of cultural heritage preservation due to their role in biodeterioration phenomena. Interestingly, fungi belonging to *Hypocreales* are frequently recovered during studies on heritage sites. This study investigates the diversity of fungal species belonging to four families in *Hypocreales.* These samples are taken from a pool of strains recovered during various studies performed on cultural heritage sites between 2004 and 2022. The 79 strains studied had been isolated from 20 different sites located in France and Belgium. Most of these sites were Paleolithic decorated caves. The multi-locus phylogenetic analysis of these strains through maximum likelihood and Bayesian inference revealed that the strains mainly belonged to the *Cordycipitaceae* family. Of the remaining strains, some belonged to *Clavicipitaceae*, *Ophiocordycipitaceae* or *Bionectriaceae*, and others were classed as *Hypocreales* but could not be placed in any existing families within this order. This study led to the description of ten new species and two new genera, i.e. *Frescium gen. nov.* and *Lenticillium gen. nov.* Species in *Hypocreales* are mainly known to be pathogenic and are mostly entomopathogenic in the case of the *Cordycipitaceae* family. In the light of this knowledge, our study also seeks to evaluate how the presence of the fungal species could indicate the presence of their hosts. Indeed, arthropod-mediated fungal dissemination is an emerging question in the domain of cultural heritage preservation.

Citation: Leplat J, François A, Bousta F (2026). Diversity of fungal species belonging to *Hypocreales* and recovered in a cultural heritage environment, with an emphasis on Paleolithic decorated caves. *Fungal Systematics and Evolution* **17**: 184–220.
Received: 16 March 2026; **Accepted:** 8 May 2026; **Effectively published online:** 12 June 2026
Corresponding editor: P.W. Crous

INTRODUCTION

Fungi are a predominant factor when studying biodeterioration phenomena in the cultural heritage environment (Sterflinger 2010). These organisms can not only be a threat for cultural heritage objects kept indoors in museums and archives (Pangallo *et al.* 2009, Pinheiro *et al*. 2019), but also damage the monuments themselves by growing on painted and unpainted walls, both indoors and out (Scheerer *et al.* 2009, De Leo *et al.* 2022, Zucconi *et al.* 2022). In this context, collections designed to isolate or count the fungal strains responsible for such deterioration can take several forms, including surface samplings and air samplings (Rojas *et al.* 2012, Pasquarella *et al.* 2015). These collections can also be performed during routine monitoring for the prevention of fungal contaminations and can thus shape decisions to improve heritage management. One such example is the discovery of the fungal outbreak that occurred in the emblematic Paleolithic decorated cave of Lascaux, leading to the decision to search for early indicators of any risk of fungal development in these particular environments (Bastian & Alabouvette 2009). The use of these indicators requires an understanding of the healthy microbial behaviour of caves before the damage occurs; a reliable knowledge of normal cave behaviour is a prerequisite to identifying potential imbalance. Several long-term surveys have been in progress over the past decade to determine whether models of aerobiological behaviour could be identified in several caves of different sizes, ranging from rock shelters to large caves that are open or closed to the public (Leplat *et al.* 2019, 2020b).

These surveys highlight the influence of the external environment on the aerobiological behaviour of caves. Small caves are strongly affected by the exterior environment along their entire length, while larger caves are generally affected by the exterior environment at their entry but much less so at locations further inside, as previously noted in other studies (Docampo *et al*. 2011, Mulec *et al*. 2012). In the areas that are mainly influenced by the exterior environment, *Cladosporium* and *Penicillium* were the dominant fungal genera. These genera are ubiquitous (Bensch *et al.* 2012, Yadav *et al.* 2018), and are therefore not characteristic of the cave environment. During these surveys, we also isolated many fungal species belonging to *Hypocreales*, and especially to *Cordycipitaceae*, which could be far more characteristic of a cave environment. The fungi belonging to this order are characterized by highly diverse lifestyles, including pathogenic ones (Perera *et al.* 2023). The presence of these fungi could therefore provide data pertaining to the presence of their hosts in the environment. For example, *Cordycipitaceae* and *Ophiocordycipitaceae* are known to contain species that are animal pathogens (mainly arthropods), and other species that are fungicolous, while *Clavicipitaceae* is known to contain species associated with plant and animal pathogens (Spatafora *et al.* 2007, Zhang *et al.* 2018). Considering

that arthropods are abundant in caves and that troglobiont species are obligate species in subterranean spaces (Culver & Pipan 2018, Mammola *et al*. 2022), it is not surprising that many arthropod-pathogenic fungal species are recovered in such environments.

The role of the fungi / arthropod association has become an important question in the context of cultural heritage biodeterioration. Indeed, arthropods are now considered to be a possible source of fungal dispersion in monuments (Jurado *et al.* 2008, Trovão *et al.* 2013). In the case of the fungal outbreak that occurred in the Lascaux cave, studies showed that *Folsomia candida* (*Collembola*) could be involved in the dissemination of black stains on the cave walls (Bastian *et al.* 2010, Alonso *et al.* 2022). Black stains represent a source of nutrients for *F. candida,* which then disseminate the fungi through their faeces. Other studies also suggested that certain arthropod species that are known to be responsible for biodeterioration, especially that of wood and paper, can also feed on fungi and be attracted by the latter (Green 2008, Pinzari 2011). Conversely, arthropods can also represent a source of nutrients for fungi. For example, entomogenous fungi are able to grow on arthropod cadavers (Jurado *et al.* 2009). Remains resulting from arthropod activity, such as metabolic water, fragmented debris and droppings, can also be favourable substrates for fungal development (Sterflinger & Pinzari 2012).

The aim of this study was therefore to evaluate the diversity of hypocrealean fungi recovered in cultural heritage sites, with an emphasis on fungi recovered in Paleolithic decorated caves. The strains studied in this paper are those collected over several years during different surveys in the framework of cultural heritage preservation. The study also sought to consider based on bibliographic data how far the presence of a given species could indicate the presence of their host in the cultural heritage environment.

MATERIALS AND METHODS

Fungal strains studied

This study considered 79 strains isolated between 2004 and 2022 in 20 different cultural heritage sites in France and Belgium (Table 1). Sixty-eight of the strains were isolated from 14 different Paleolithic decorated caves or shelters, seven were isolated from religious monuments, two were isolated from a flint mine and two were isolated from a museum (Fig. 1). Fifty-three of the strains were isolated through air samplings, 20 were isolated through surface samplings and six were isolated from soil samplings. Briefly, air samplings were collected with a Duo SAS Super 360 air sampler (VWR-pbi, Milan, Italy) containing malt extract agar (MEA; Merck KGaA, Darmstadt, Germany) culture medium in 55 mm Petri dishes. Surface samplings were made with sterile swabs, then inoculated on MEA. Strains from soil sampling were obtained by serial dilution of 1 g of soil in sterile water, followed by inoculation on MEA. The most frequent combination between type of place sampled and sampling type was air sampling in Paleolithic decorated caves (51 strains). All the strains recovered from religious monuments and the museum were isolated through surface sampling while the two strains recovered in the flint mine were isolated through air sampling.

The strains were then preserved on MEA in Sabouraud-2 % dextrose broth (Merck KGaA, Darmstadt, Germany) supplemented with 20 % glycerol at -84 °C. In addition, the holotype of each new species described through both phylogenetic and morphologic analysis in this study was included in the CBS culture collection (Westerdijk Institute, Utrecht, The Netherlands).

Phylogenetic study

Reference strains: The reference strains were chosen to cover the known *Hypocreales* diversity as exhaustively as possible. Thus, the phylogeny of the isolated strains was studied at three levels to determine their taxonomy. First, the strains were studied at the order level to assign them into the different *Hypocreales* families. One species of each genus composing *Hypocreales* was used in this first study. The strains were then studied at the family level to assign them to the different genera. Two species of each genus composing the family were used in these studies. Finally, the strains were studied at the genus level to assign them to the different species. Two strains of each species composing the genus were used in these final studies.

In general, the study only included strains for which sequences from at least two different DNA loci were available in the NCBI GenBank database (Clark *et al.* 2016). In rare cases of species or genera for which very few sequences appear in GenBank, strains with only one DNA locus sequence available were included in the reference set (Table S1).

DNA extraction, PCR amplification and sequencing: Fungal DNA was extracted as described by Edel *et al.* (2001). Primer pairs described in Table 2 were used to amplify the nuclear ribosomal internal transcribed spacer (ITS) region, the large subunit of nuclear-encoded ribosomal DNA (nrLSU), the translation elongation factor 1-alpha gene (*tef-1α*), the largest subunit of RNA polymerase II (*rpb1*) and the second largest subunit of RNA polymerase II (*rpb2*). PCR was performed in 25 µL reaction volumes, with 1 µL of template DNA, 1 U of Taq DNA polymerase (Invitrogen, Carlsbad, USA), 2.5 µL of 10X Taq DNA polymerase buffer, 1 µL of 2 mmol/L dNTPs (0.08 mmol/L final; Thermo Fisher Scientific, Waltham, USA) and 1.5 µL of each 10 µmol/L primer (0.6 mmol/L final; Eurogentec, Seraing, Belgium). Amplifications were performed on a VeritiPro thermocycler (Applied Biosystems, Waltham, USA) using the following parameters: a 5 min step at 95 °C, followed by 35 cycles of 1 min at 95 °C, 1 min at the appropriate annealing temperature provided in Table 2 for each primer pair, 1 min at 72 °C, and a final 10 min extension step at 72 °C. PCR products were sequenced by Genoscreen (Lille, France) using the same primer set. Generated sequences were submitted to the NCBI GenBank database.

Sequence alignment and phylogenetic analyses: The sequences generated in this study were verified with BioEdit v. 7.2.5 (Hall 1999). The sequences related to reference strains were downloaded from the NCBI GenBank database. In the case of strains for which GenBank provided the whole genome but lacked the sequences for the specific region studied, the sequences were extracted from the whole genome via the MAFFT v. 7 web server, using the sequence

Table 1. Description of fungal strains studied.

Species	Collection number	Sampling place	Sampling date	Sampling method	Previous study referring to the strain
Amphichorda excrementa	LRMH C158, CBS 150563	Bayol cave (Collias, Occitanie, France)	Sep-15	Soil sampling	—
Beauveria bassiana	LRMH C550	Cap-Blanc shelter (Marquay, Nouvelle-Aquitaine, France)	Oct-21	Air sampling	—
Beauveria caledonica	LRMH C222	La Mouthe cave (Les Eyzies-de-Taillac-Sireuil, Nouvelle-Aquitaine, France)	Oct-16	Air sampling	—
Beauveria namnaoensis / peruviensis	LRMH C294	Chauvet cave, (Vallon-Pont-d'Arc, Auvergne-Rhône-Alpes, France)	Oct-18	Surface sampling	—
Beauveria pseudobassiana	LRMH C272	Chauvet cave, (Vallon-Pont-d'Arc, Auvergne-Rhône-Alpes, France)	May-17	Air sampling	—
	LRMH C292	Points Cave (Aiguèze, Occitanie, France)	May-17	Air sampling	—
	LRMH C305	Font-de-Gaume cave (Les Eyzies-de-Taillac-Sireuil, Nouvelle-Aquitaine, France)	Oct-18	Air sampling	—
	LRMH C324	Chauvet cave, (Vallon-Pont-d'Arc, Auvergne-Rhône-Alpes, France)	Jan-19	Surface sampling	—
	LRMH C332	Chauvet cave, (Vallon-Pont-d'Arc, Auvergne-Rhône-Alpes, France)	Jan-19	Surface sampling	—
	LRMH C544	Combarelles cave (Les Eyzies-de-Taillac-Sireuil, Nouvelle-Aquitaine, France)	Oct-21	Air sampling	—
Beauveria varroae	LRMH C291	Chauvet cave, (Vallon-Pont-d'Arc, Auvergne-Rhône-Alpes, France)	May-17	Air sampling	—
Cordyceps fumosorosea	LRMH C136	Combarelles cave (Les Eyzies-de-Taillac-Sireuil, Nouvelle-Aquitaine, France)	Aug-15	Air sampling	—
	LRMH C181	Chabot cave (Aiguèze, Occitanie, France)	Jun-16	Air sampling	—
	LRMH C275	Chauvet cave, (Vallon-Pont-d'Arc, Auvergne-Rhône-Alpes, France)	May-17	Air sampling	—
	LRMH C379	Baume Latrone cave (Sainte-Anastasie, Occitanie, France)	Jul-20	Air sampling	—
Corniculantispora dimorpha	LRMH C342	Cosquer cave (Marseille, Provence-Alpes-Côte d'Azur, France)	Jul-19	Air sampling	—
Corniculantispora psalliotae	LRMH C051	Lascaux cave (Montignac-Lascaux, Nouvelle-Aquitaine, France)	Mar-04	Soil sampling	—
Corniculantispora pseudoaranearum sp. nov.	LRMH C177	Chabot cave (Aiguèze, Occitanie, France)	Jun-16	Air sampling	—
	LRMH C250, CBS 150564	Font-de-Gaume cave (Les Eyzies-de-Taillac-Sireuil, Nouvelle-Aquitaine, France)	Oct-16	Air sampling	—
Engyodontium latronense sp. nov.	LRMH C469, CBS 150569	Baume Latrone cave (Sainte-Anastasie, Occitanie, France)	Jul-21	Air sampling	—
Frescium cyprienense sp. nov.	LRMH C122, CBS 150562	Crypt of Saint-Savin-sur-Gartempe Abbey-church (Nouvelle-Aquitaine, France)	Nov-15	Surface sampling	(Leplat *et al.* 2017)
Frescium savinense sp. nov.	LRMH C121, CBS 150561	Crypt of Saint-Savin-sur-Gartempe Abbey-church (Nouvelle-Aquitaine, France)	Nov-15	Surface sampling	(Leplat *et al.* 2017)
Gamszarea cavernicola sp. nov.	LRMH C231	Cap-Blanc shelter (Marquay, Nouvelle-Aquitaine, France)	Oct-16	Surface sampling	—
	LRMH C246	Pair-non-Pair cave (Prignac-et-Marcamps, Nouvelle-Aquitaine, France	Oct-16	Air sampling	—
	LRMH C326, CBS 150567	Chauvet cave, (Vallon-Pont-d'Arc, Auvergne-Rhône-Alpes, France)	Jan-19	Surface sampling	—
Gamszarea microspora	LRMH C331	Chauvet cave, (Vallon-Pont-d'Arc, Auvergne-Rhône-Alpes, France)	Jan-19	Surface sampling	—
Lenticillium mouthense sp. nov.	LRMH C311, CBS 150566	La Mouthe cave (Les Eyzies-de-Taillac-Sireuil, Nouvelle-Aquitaine, France)	Oct-18	Air sampling	—
Leptobacillium cavernicola	LRMH C212	Pech Merle cave (Cabrerets, Occitanie, France)	Oct-16	Air sampling	(Leplat *et al.* 2022b)

	LRMH C216	Pech Merle cave (Cabrerets, Occitanie, France)	Oct-16	Air sampling	(Leplat *et al.* 2022b)
	LRMH C217	Pair-non-Pair cave (Prignac-et-Marcamps, Nouvelle-Aquitaine, France)	Oct-16	Air sampling	(Leplat *et al.* 2022b)
	LRMH C248	Pair-non-Pair cave (Prignac-et-Marcamps, Nouvelle-Aquitaine, France	Oct-16	Air sampling	(Leplat *et al.* 2022b)
	LRMH C251	Font-de-Gaume cave (Les Eyzies-de-Taillac-Sireuil, Nouvelle-Aquitaine, France)	Oct-16	Air sampling	(Leplat *et al.* 2022b)
	LRMH C299, CBS 149113	Pair-non-Pair cave (Prignac-et-Marcamps, Nouvelle-Aquitaine, France	Oct-18	Surface sampling	(Leplat *et al.* 2022b)
	LRMH C302 CBS 149234	Pech Merle cave (Cabrerets, Occitanie, France)	Oct-18	Air sampling	(Leplat *et al.* 2022b)
	LRMH C304	Pech Merle cave (Cabrerets, Occitanie, France)	Oct-18	Air sampling	(Leplat *et al.* 2022b)
	LRMH C312	Combarelles cave (Les Eyzies-de-Taillac-Sireuil, Nouvelle-Aquitaine, France)	Oct-18	Air sampling	(Leplat *et al.* 2022b)
	LRMH C313	Combarelles cave (Les Eyzies-de-Taillac-Sireuil, Nouvelle-Aquitaine, France)	Oct-18	Air sampling	(Leplat *et al.* 2022b)
	LRMH C314	Combarelles cave (Les Eyzies-de-Taillac-Sireuil, Nouvelle-Aquitaine, France)	Oct-18	Air sampling	(Leplat *et al.* 2022b)
Metapochonia suchlasporia var. *suchlasporia*	LRMH C046	Lascaux cave (Montignac-Lascaux, Nouvelle-Aquitaine, France)	Mar-04	Soil sampling	—
	LRMH C277	Chauvet cave, (Vallon-Pont-d'Arc, Auvergne-Rhône-Alpes, France)	May-17	Air sampling	—
	LRMH C298	Chauvet cave, (Vallon-Pont-d'Arc, Auvergne-Rhône-Alpes, France)	Jan-19	Surface sampling	—
Metarhizium chabotense sp. nov.	LRMH C146	Chabot cave (Aiguèze, Occitanie, France)	Sep-15	Soil sampling	—
	LRMH C192	Chabot cave (Aiguèze, Occitanie, France)	Jun-16	Air sampling	—
	LRMH C282, CBS 150565	Chabot cave (Aiguèze, Occitanie, France)	May-17	Air sampling	—
Parengyodontium album	LRMH C120	Crypt of Saint-Savin-sur-Gartempe Abbey-church (Nouvelle-Aquitaine, France)	Nov-15	Surface sampling	(Leplat *et al.* 2017, 2022a)
	LRMH C267	Bastia museum (Corse, France)	Dec-16	Surface sampling	(Leplat *et al.* 2022a)
	LRMH C268	Bastia museum (Corse, France)	Dec-16	Surface sampling	(Leplat *et al.* 2022a)
	LRMH C327	Chauvet cave, (Vallon-Pont-d'Arc, Auvergne-Rhône-Alpes, France)	Jan-19	Surface sampling	(Leplat *et al.* 2022a)
	LRMH C343	Cosquer cave (Marseille, Provence-Alpes-Côte d'Azur, France)	Jul-19	Air sampling	(Leplat *et al.* 2022a)
	LRMH C345	Cosquer cave (Marseille, Provence-Alpes-Côte d'Azur, France)	Jul-19	Air sampling	(Leplat *et al.* 2022a)
	LRMH C346	Cosquer cave (Marseille, Provence-Alpes-Côte d'Azur, France)	Jul-19	Air sampling	(Leplat *et al.* 2022a)
	LRMH C349	Cosquer cave (Marseille, Provence-Alpes-Côte d'Azur, France)	Jul-19	Air sampling	(Leplat *et al.* 2022a)
	LRMH C350	Cosquer cave (Marseille, Provence-Alpes-Côte d'Azur, France)	Jul-19	Air sampling	(Leplat *et al.* 2022a)
	LRMH C355	Cosquer cave (Marseille, Provence-Alpes-Côte d'Azur, France)	Jul-19	Air sampling	(Leplat *et al.* 2022a)
	LRMH C358	Cosquer cave (Marseille, Provence-Alpes-Côte d'Azur, France)	Jul-19	Air sampling	(Leplat *et al.* 2022a)
	LRMH C451	Points Cave (Aiguèze, Occitanie, France)	Jul-21	Air sampling	—
	LRMH C466	Baume Latrone cave (Sainte-Anastasie, Occitanie, France)	Jul-21	Air sampling	—
	LRMH C467	Baume Latrone cave (Sainte-Anastasie, Occitanie, France)	Jul-21	Air sampling	—
	LRMH C468	Baume Latrone cave (Sainte-Anastasie, Occitanie, France)	Jul-21	Air sampling	—

	LRMH C579	Tapestry preserved in the Abbey of La Chaise-Dieu, Auvergne-Rhône-Alpes, France	Jun-22	Surface sampling	—
	LRMH C581	Tapestry preserved in the Abbey of La Chaise-Dieu, Auvergne-Rhône-Alpes, France	Jun-22	Surface sampling	—
Parengyodontium torokii	LRMH C057	Lascaux cave (Montignac-Lascaux, Nouvelle-Aquitaine, France)	Dec-04	Air sampling	(Leplat *et al*. 2022a)
	LRMH C133	Chauvet cave, (Vallon-Pont-d'Arc, Auvergne-Rhône-Alpes, France)	Mar-16	Air sampling	(Leplat *et al*. 2022a)
	LRMH C243, CBS 149111	Pair sampling-non-Pair sampling cave (Prignac-et-Marcamps, Nouvelle-Aquitaine, France)	Oct-16	Air sampling	(Leplat *et al*. 2022a)
	LRMH C325, CBS 149112	Chauvet cave, (Vallon-Pont-d'Arc, Auvergne-Rhône-Alpes, France)	Jan-19	Surface sampling	(Leplat *et al*. 2022a)
	LRMH C356	Cosquer cave (Marseille, Provence-Alpes-Côte d'Azur, France)	Jul-19	Air sampling	(Leplat *et al*. 2022a)
	LRMH C357	Cosquer cave (Marseille, Provence-Alpes-Côte d'Azur, France)	Jul-19	Air sampling	(Leplat *et al*. 2022a)
	LRMH C364	Pigeonnier cave (Domme, Nouvelle-Aquitaine, France)	Oct-16	Air sampling	(Leplat *et al*. 2022a)
	LRMH C450	Points Cave (Aiguèze, Occitanie, France)	Jul-21	Air sampling	—
	LRMH C627	Flint mines of Spiennes (Mons, Wallonia, Belgium)	Jun-22	Air sampling	—
Purpureocillium lavendulum	LRMH C102	Hypogée des Dunes (Poitiers, Nouvelle-Aquitaine, France)	Mar-13	Surface sampling	—
Samsoniella cardinalis	LRMH C135	Flint mines of Spiennes (Mons, Wallonia, Belgium)	Jun-16	Air sampling	—
Samsoniella hepiali	LRMH C048	Lascaux cave (Montignac-Lascaux, Nouvelle-Aquitaine, France)	Mar-04	Soil sampling	—
Simplicillium aogashimaense	LRMH C568	Saint-Joseph Chapel of Ars-sur-Formans (Auvergne-Rhône-Alpes, France)	Feb-22	Surface sampling	—
Simplicillium aquitainense sp. nov.	LRMH C159	Baume Latrone cave (Sainte-Anastasie, Occitanie, France)	Sep-15	Soil sampling	—
	LRMH C300, CBS 150708	Pair-non-Pair cave (Prignac-et-Marcamps, Nouvelle-Aquitaine, France	Oct-18	Surface sampling	—
Simplicillium neosympodiophorum sp. nov.	LRMH C195	Baume Latrone cave (Sainte-Anastasie, Occitanie, France)	Jun-16	Air sampling	—
	LRMH C465, CBS 150568	Baume Latrone cave (Sainte-Anastasie, Occitanie, France)	Jul-21	Air sampling	—
Simplicillium pechmerlense	LRMH C241, CBS 147188	Pech Merle cave (Cabrerets, Occitanie, France)	Oct-16	Air sampling	(Leplat *et al*. 2021)

Table 2. Primers used to amplify fungal strains in this study.

Target gene	Primer	Primer DNA sequence	Annealing temperature	Reference
ITS	ITS1-F	CTTGGTCATTTAGAGGAAGTAA	50°C	(Gardes & Bruns 1993)
	ITS4	TCCTCCGCTTATTGATATGC		(White *et al.* 1990)
LSU	LR0R	GTACCCGCTGAACTTAAGC	56 °C	(Vilgalys & Hester 1990)
	LR5	ATCCTGAGGGAAACTTC		
tef-1α	983F	GCYCCYGGHCAYCGTGAYTTYAT	55 °C	(Rehner & Buckley 2005)
	2218R	ATGACACCRACRGCRACRGTYTG		
rpb1	CRPB1	CCWGGYTTYATCAAGAARGT	55 °C	(Castlebury *et al.* 2004)
	RPB1Cr	CCNGCDATNTCRTTRTCCATRTA		(Matheny *et al.* 2002)
rpb2	fRPB2-5f	GAYGAYMGWGATCAYTTYGG	58 °C	(Liu *et al.* 1999)
	fRPB2-7cR	CCCATRGCTTGYTTRCCCAT		

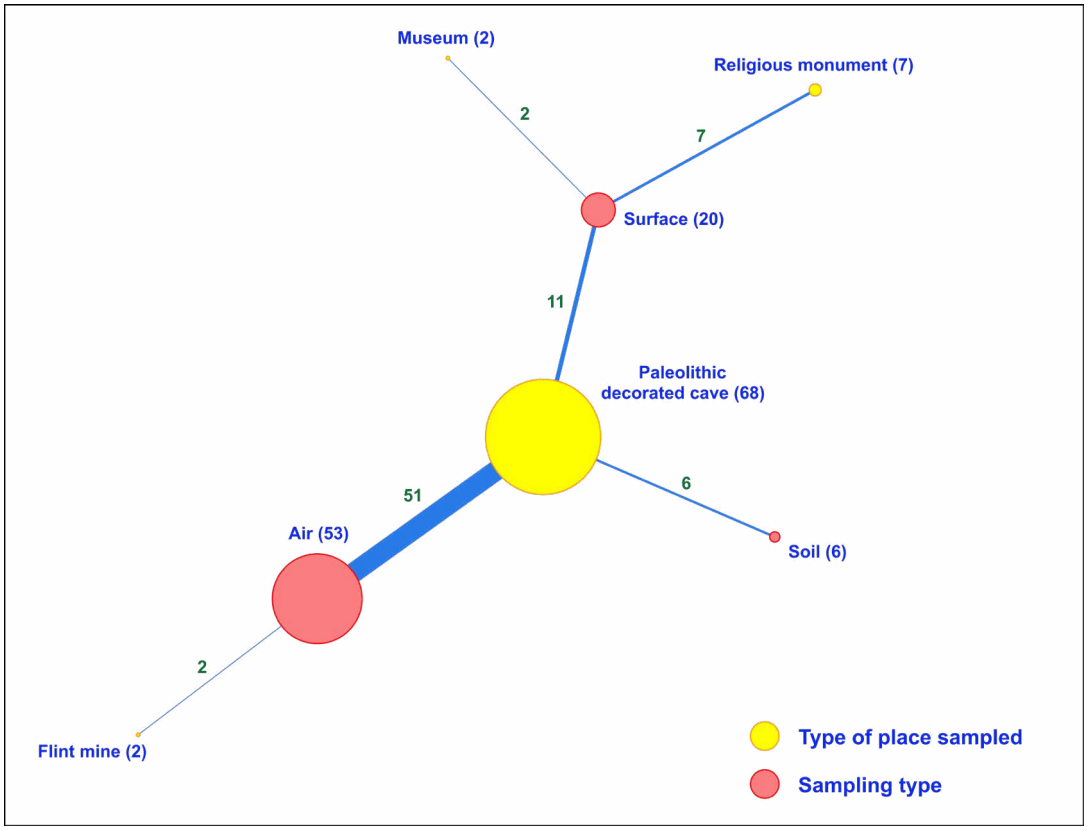

Fig. 1. Description of the sampling data of the studied strains. The figure depicts the type of place in which the studied strains were isolated and the sampling method through a network representation. The size of the nodes and that of the vertices is proportional to the number of relevant fungal strains. The numbers attributed to each node and to each vertex correspond to the number of relevant fungal strains.

of the closest species as a reference (Katoh *et al.* 2019). Multiple sequence alignments for each DNA region studied were performed using the FFT-NS-i alignment strategy from the MAFFT web server. Uninformative gaps and ambiguous regions were removed using the Gblocks program v. 0.91.1 implemented in the NGPhylogeny.fr service, with the program set for a lightly stringent selection (minimum number of sequences for a conserved position: 50 % of the sequences + 1; minimum length of a block: 5; allowed gap position: "with half"; (Talavera & Castresana 2007, Lemoine *et al.* 2019). The maximum likelihood (ML) analysis of concatenated regions was performed using the graphical interface of RAxML v. 8 set to 1000 thorough bootstrap iterations, and the GTRGAMMA substitution model (Stamatakis 2014, Edler *et al.* 2021). Bayesian inference (BI) analysis of concatenated regions was performed using MrBayes v. 3.2.7a implemented in PhyloSuite v. 1.2.3, based on a Markov Monte Carlo Chain (MCMC) set to two simultaneously executed runs for 10 M generations with the GTRGAMMA substitution model (Ronquist *et al.* 2012, Xiang *et al.* 2023). Trees were sampled every 1000 generations, with the burn-in fraction set to 25 %. Trees were generated using MEGA v. 12 (Kumar *et al.* 2024). Then, generated trees were edited using Inkscape v. 1.4.2.

All alignments and all trees generated during the study were deposited in the TreeBASE (Piel *et al.* 2000), under submission number 32410.

Morphological study

The macroscopic features, including the size, colour (Kornerup & Wanscher 1967), morphology and pigment production of each of the studied strains, were assessed on MEA and on potato dextrose agar (PDA; VWR International, Radnor, USA) after a 10 d incubation at 25 °C and 30 °C in the dark. Microscopic features, including the size and the shape of conidiogenous cells and conidia, were assessed on MEA after a 14 d incubation at 25 °C. After treatment with Shear's mounting fluid (Crous *et al.* 2009), observations were performed in differential interference contrast microscopy (DIC) with an Axio Observer microscope (Zeiss, Oberkochen, Germany). Microscopic features were captured with a C11440-42U40 camera (Hamamatsu photonics, Hamamatsu City, Japan) using the ZEN program (Zeiss, Oberkochen, Germany).

RESULTS

Through phylogenetic analysis at the order level, the studied strains were sorted into the different families belonging to *Hypocreales*. Of the 79 strains, one was placed in *Bionectriaceae*, 68 in *Cordycipitaceae*, six in *Clavicipitaceae*, one in *Ophiocordycipitaceae*, and three strains could not be placed with any certainty into any family (Table 3, Figs 2, S1).

The strain sorted in *Bionectriaceae* was identified as an *Amphichorda* species (Table 3, Figs 2, S2); and more precisely as *A. excrementa* (Table 3, Fig. S3).

Phylogenetic analysis in *Cordycipitaceae* attributed the studied strains between the *Beauveria*, *Cordyceps*, *Corniculantispora*, *Engyodontium*, *Gamszarea*, *Leptobacillium*, *Parengyodontium*, *Samsoniella* and *Simplicillium* genera (Table 3, Figs 2, S4). This study also highlighted the need for new combinations with regards to some previously described species. The highest number of isolated strains were placed in *Parengyodontium* (26

Table 3. Size and composition of the matrix for the different phylogenetic studies.

Level of the study	Number of taxa	Size of the concatenated alignment (bp)	Size DNA regions (bp)					Corresponding figure
			ITS	nrLSU	*rpb1*	*rpb2*	*tef-1α*	
Hypocreales	363	3268	300	804	547	675	942	Fig. S1
Bionectriaceae	78	3515	431	825	698	754	807	Fig. S2
Amphichorda	20	3971	519	829	682	1024	875	Fig. S3
Cordycipitaceae	146	4038	513	851	681	1032	961	Fig. S4
Beauveria	82	3658	513	784	560	913	888	Fig. S5
Cordyceps	128	3992	538	862	771	956	925	Fig. S6
Corniculantispora	11	4071	540	831	675	1026	957	Fig. 3
Engyodontium	8	3780	543	561	705	1041	930	Fig. 4
Gamszarea	21	4014	546	831	702	1026	909	Fig. 5
Leptobacillium	31	4041	513	834	678	1050	966	Fig. S7
Parengyodontium	35	4065	558	858	684	1005	960	Fig. S8
Samsoniella	84	4089	567	861	717	987	957	Fig. S9
Simplicillium	63	3969	525	816	690	1026	912	Fig. 6
Clavicipitaceae	93	3924	454	830	662	1047	911	Fig. S10
Metapochonia	23	3993	513	828	681	1029	942	Fig. S11
Metarhizium	120	3645	483	816	630	821	894	Fig. 7
Ophiocordycipitaceae	15	3973	554	859	668	969	923	Fig. S12
Purpureocillium	19	4008	528	846	678	1026	930	Fig. S13
Families related to *Frescium* genus	326	3614	364	787	681	872	910	Fig. 8
Families related to *Lenticillium* genus	337	3718	338	800	676	931	918	Fig. 9

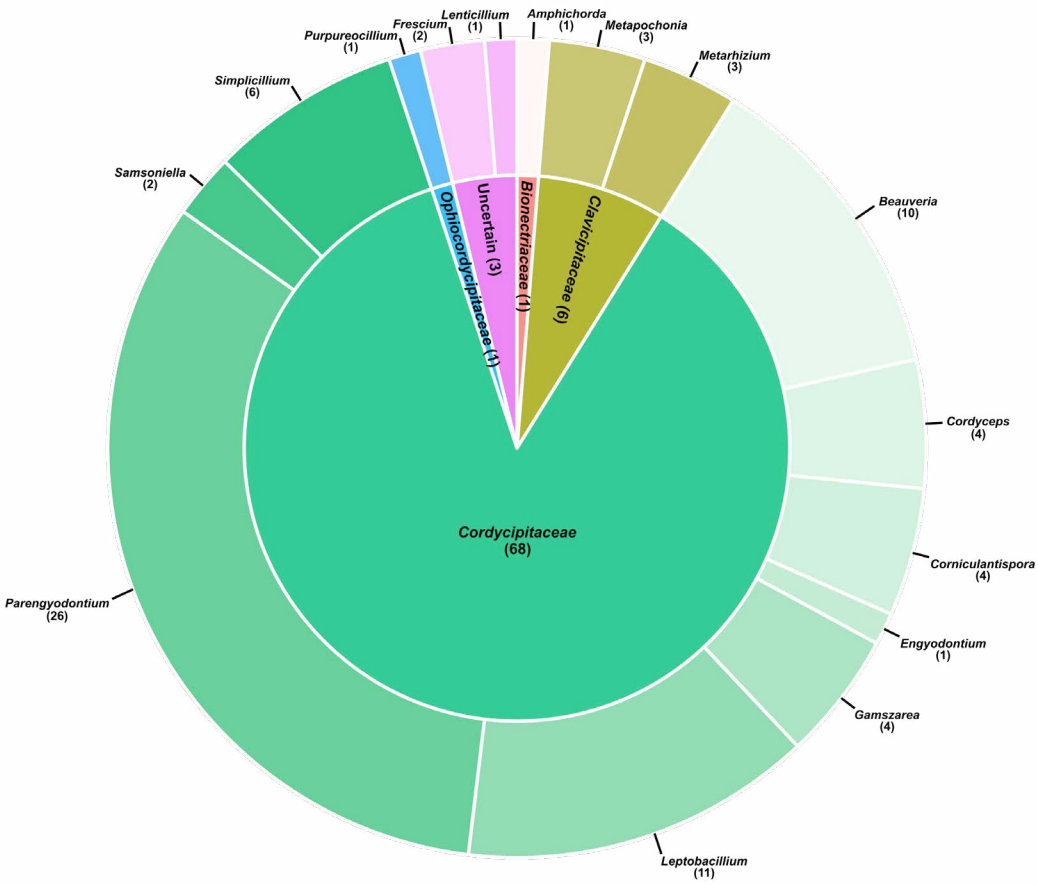

Fig. 2. Sorting of the studied strains in families and genera among *Hypocreales*. The 79 studied strains were depicted in a "PieDonut" chart. The first level of the chart represents the family level, and the second level represents the genus level. The size of each chart section is proportional to the number of strains sorted in that specific section.

strains), while only one strain belonged to *Engyodontium*. All the species identified in the genera *Beauveria*, *Cordyceps*, *Leptobacillium*, *Parengyodontium* and *Samsoniella* corresponded to known species, while new species were described from the strains placed in *Corniculantispora*, *Engyodontium*, *Gamszarea* and *Simplicillium*: one new species was described in each of these genera with the exception of *Simplicillium,* in which two new species were described (Table 3, Figs 3–6, S5–S9). In addition, new combinations were proposed for three previously described species: one species was transferred to *Engyodontium* and two to *Gamszarea*.

Among the six strains identified as *Clavicipitaceae*, three were placed in *Metapochonia* and the three others were placed in *Metarhizium* (Table 3, Figs 2, S10). The three *Metapochonia* strains were identified as *M. suchlasporia* var. *suchlasporia* (Table 3, Fig. S11), while the three *Metarhizium* strains were described as the new species *M. chabotense* (Table 3, Fig. 7).

The strain placed in *Ophiocordycipitaceae* was identified as a *Purpureocillium* species (Table 3, Figs 2, S12); and more precisely as *P. lavendulum* (Table 3, Fig. S13).

Among the three strains that could not be allocated to any family, two were phylogenetically related to each other with closest correspondences to *Clavicipitaceae*, *Cordycipitaceae*, *Hypocreaceae*, *Nectriaceae*, *Ophicordycipitaceae* or *Valsonectriaceae* depending on the DNA locus considered (Table 3, Fig. S1); the third strain was not related to the two others, and its closest relationships were found in *Calcarisporiaceae*, *Clavicipitaceae*, *Cordycipitaceae*, *Hypocreaceae*, *Nectriaceae*, *Ophicordycipitaceae*, *Polycephalomycetaceae* or *Pseudodiploosporaceae* depending on the DNA locus considered. Following the study of these strains in relation to the closest *Hypocreales* families determined by the study of single DNA loci, *Frescium* and *Lenticillium* were described as new genera (Table 3, Figs 8, 9).

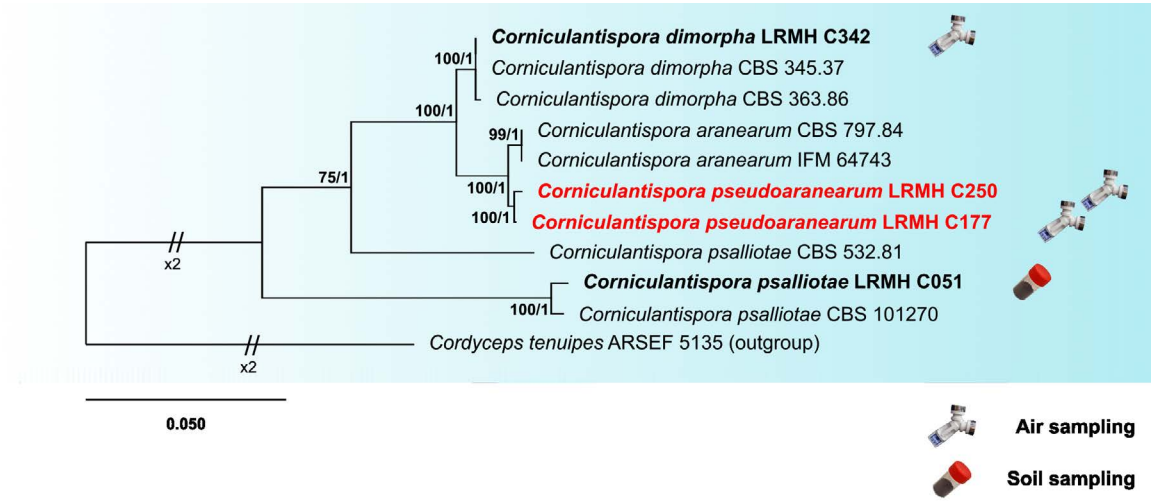

Fig. 3. Phylogenetic studies through maximum likelihood (ML) and Bayesian inference (BI) among *Corniculantispora* species. The trees were rooted with *Cordyceps tenuipes* ARSEF 5135 (*Cordycipitaceae*) as an outgroup. Bootstrap values greater than or equal to 70 % and Bayesian posterior probabilities greater than or equal to 0.70 are located close to the corresponding nodes. The studied strains are displayed in bold print. The newly described species from studied strains are displayed in bold red print.

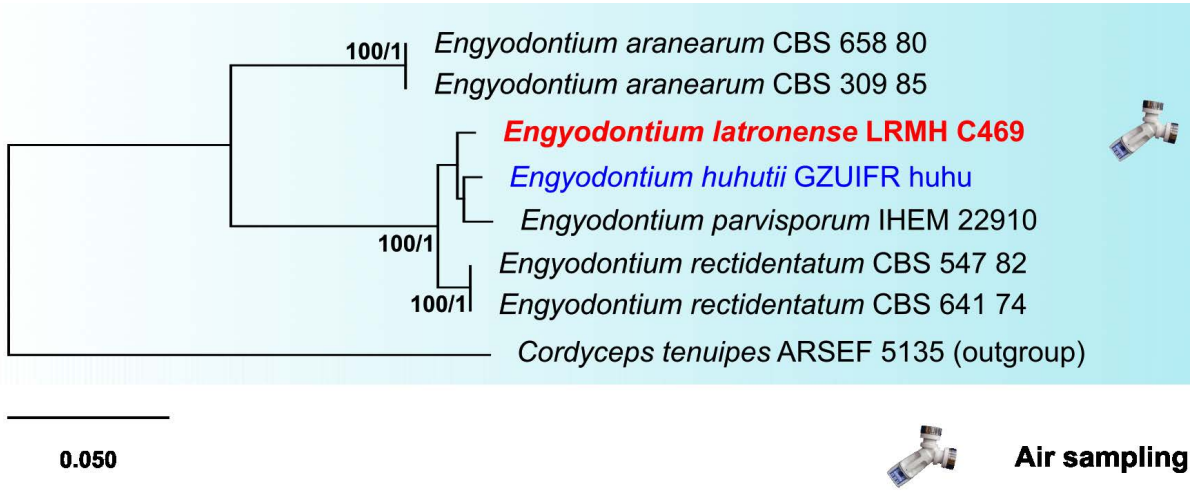

Fig. 4. Phylogenetic studies through maximum likelihood (ML) and Bayesian inference (BI) among *Engyodontium* species. The trees were rooted with *Cordyceps tenuipes* ARSEF 5135 (*Cordycipitaceae*) as an outgroup. Bootstrap values greater than or equal to 70 % and Bayesian posterior probabilities greater than or equal to 0.70 are located close to the corresponding nodes. The studied strains are displayed in bold print. The newly described species from studied strains is displayed in bold red print. The new combination of previously described species transferred into *Engyodontium* is displayed in blue print.

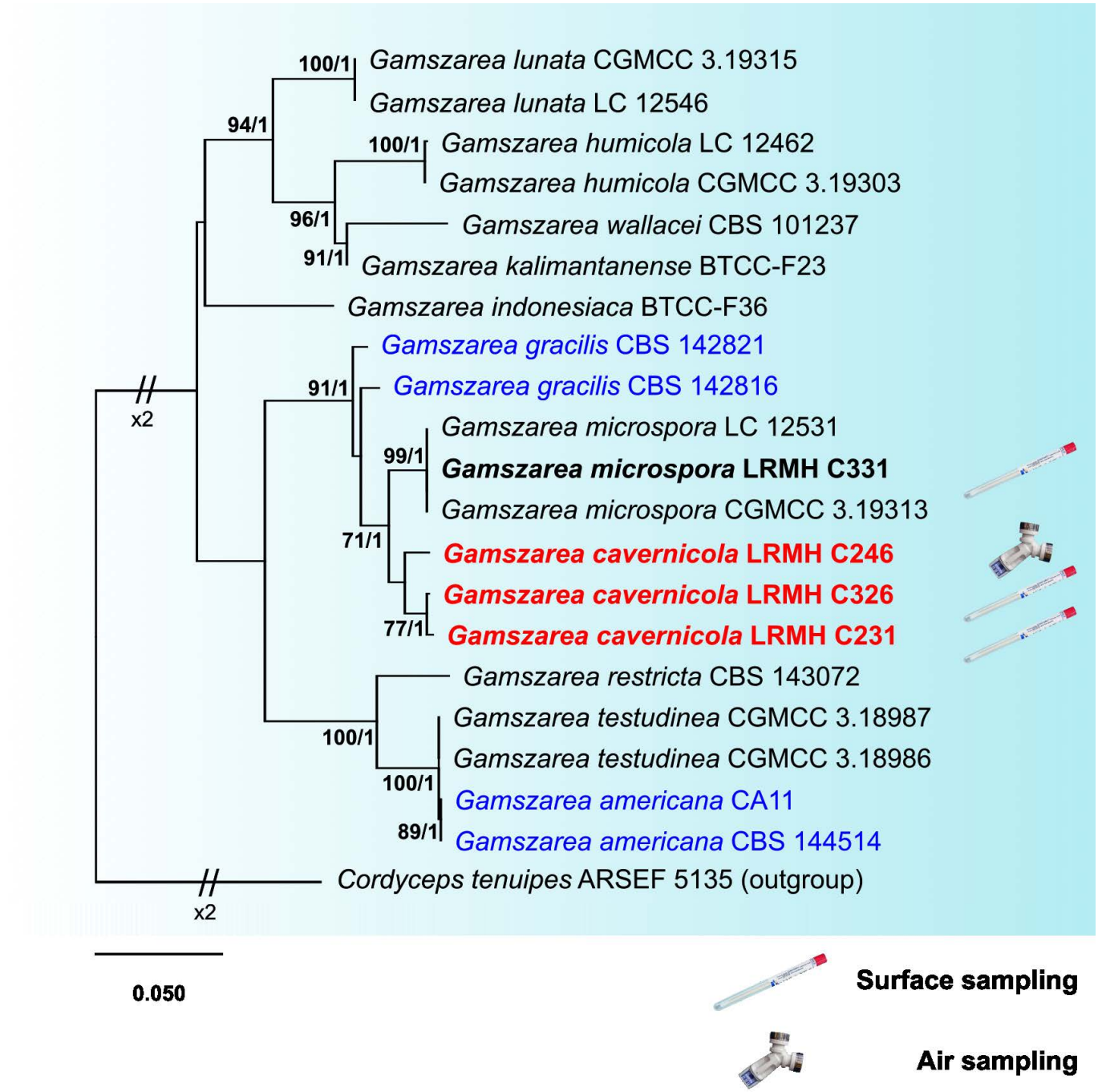

Fig. 5. Phylogenetic studies through maximum likelihood (ML) and Bayesian inference (BI) among *Gamszarea* species. The trees were rooted with *Cordyceps tenuipes* ARSEF 5135 (*Cordycipitaceae*) as an outgroup. Bootstrap values greater than or equal to 70 % and Bayesian posterior probabilities greater than or equal to 0.70 are located close to the corresponding nodes. The studied strains are displayed in bold print. Newly described species from studied strains are displayed in bold red print. New combinations of previously described species transferred into *Gamszarea* are displayed in blue print.

Taxonomy

The description of some of the following species is currently based on a single strain and an effort must be made to isolate further specimens of these species. Although the description of singleton-based species may not be considered best practice, it can be considered scientifically acceptable (Cazabonne *et al.* 2024).

Corniculantispora pseudoaranearum J. Leplat ***sp. nov.*** MB 861445. Fig. 10.

Etymology: The epithet *pseudoaranearum* refers to the proximity of the species with *C. aranearum*.

GenBank: OR264308 (ITS), OR263643 (nrLSU), OR269641 (*rpb1*), OR291074 (*rpb2*), OR291112 (*tef-1α*).

Typus: **France**, Les Eyzies-de-Taillac-Sireuil, 44°56’05”N, 1°01’44”E, Oct. 2016, isolated from air sampling in Font-de-Gaume cave, collected and isolated by the microbiologists of the French Historical Monuments Research Laboratory (**holotype** CBS 150564, preserved in a metabolically inactive state), culture ex-type CBS 150564 = LRMH C250.

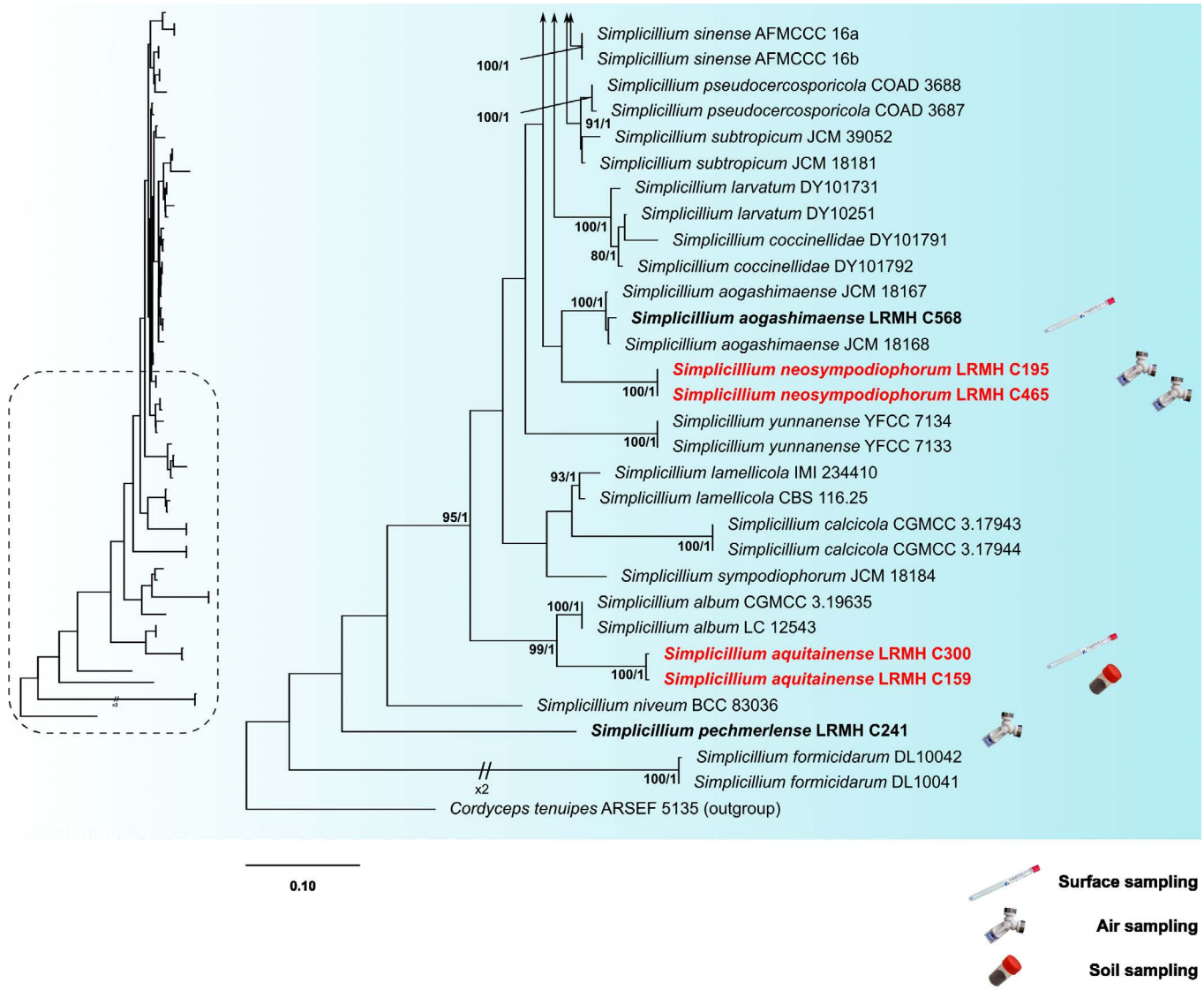

Fig. 6. Phylogenetic studies through maximum likelihood (ML) and Bayesian inference (BI) among *Simplicillium* species. The trees were rooted with *Cordyceps tenuipes* ARSEF 5135 (*Cordycipitaceae*) as an outgroup. Bootstrap values greater than or equal to 70 % and Bayesian posterior probabilities greater than or equal to 0.70 are located close to the corresponding nodes. The studied strains are displayed in bold print. Newly described species from studied strains are displayed in bold red print.

Known distribution: France, Nouvelle-Aquitaine and Occitanie regions.

Description: *Colonies* on MEA reached 54–60 mm diam. at 25 °C, white to yellowish white, floccose, production of light yellow diffusive pigment in the agar. Reverse orange. Colonies reached 50–54 mm diam. at 30 °C. Colonies on PDA reached 46–49 mm diam. after 10 d at 25 °C, white, floccose, production of greyish red diffusive pigment in the agar. Reverse greyish red. Colonies reached 56–58 mm diam. at 30 °C. *Hyphae* septate, smooth walled, hyaline. *Conidiogenous cells* arising laterally from prostrate hyphae, mainly solitary, flask shaped, tapering into a thread-like neck, 5.5–8.1 × 1.3–1.6 µm. *Conidia* aseptate, hyaline, smooth walled, solitary, ellipsoidal and apiculate, 3.8–4.9 × 1.7–2.8 µm.

Notes: The morphologic features expressed by *C. pseudoaraneaeum* are close to those expressed by *C. aranearum* (Zare & Gams 2001). The optimal growth temperature of *C. pseudoaraneaeum* seems to be higher than that observed for *C. aranearum,* since Zare & Gams (2001) found an optimal growth at 24–27 °C for *L. aphanocldii*, with no growth at 33 °C, while the growth rate of *C. pseudoaraneaeum* was higher at 30 °C than at 25 °C. The shape and size of phialides were similar in the two species, but neither the phialides arranged in pairs nor the verticillate phialides observed in *C. aranearum* were noted in *C. pseudoaraneaeum*. The shape of conidia is also similar in the two species, but conidia produced by *C. pseudoaraneaeum* seems to be slightly larger than the ones produced by *C. aranearum*. Finally, phylogenetic features clearly distinguished the two species. *Corniculantispora pseudoaranearum* and *C. aranearum* formed two sister clades, which were supported in 100 % of the bootstraps and with a posterior probability of 1.00, and in 99 % of the bootstraps with a posterior probability of 1.00 respectively (Fig. 3). These two different clades are the result of twenty-two different base pairs when considering the concatenation of ITS, nrLSU, *rpb1*, *rpb2* and *tef-1α* sequences.

Other strains examined: **France**, LRMH C177, Aiguèze 44°19'22"N, 4°32'28"E, Jun. 2016, isolated from air sampling in Chabot cave, collected and isolated by the microbiologists of the French Historical Monuments Research Laboratory.

Engyodontium huhutii J. Leplat, ***sp. nov.*** MB 849570.
[previously published as: *Lecanicillium huhutii* X. Zou & Y.M. Zhou, *Frontiers in Microbiology* **13** (no. 859886): 4. 2022, nom. inval. Art. 40.8 (Shenzhen)]

Typus: **China**, Guizhou Province: Guiyang City, Huaxi park, 5 Oct. 2013, *X. Zou & Y.M. Zhou* (**holotype** GZUIFRhuhu, preserved in a metabolically inactive state).

Description and illustration: See Zhou *et al.* (2022).

Known distribution: China. Guizhou Province: Guiyang City, Huaxi Park.

Notes: This species was first described as *Lecanicillium huhutii*. This species was considered as invalid according to Art. 40.8 (Shenzen) because the original description of the species omitted to mention that the reference culture is preserved in a metabolically inactive state. This statement has been corrected in the description of *E. huhutii*.

The authors chose to not place the species in *Engyodontium* because the latter only contained one recognized species and because the morphological features of the new species did not correspond to *Engyodontium* (Zhou *et al.* 2022). The phylogenetic study performed in the present study clearly placed this species in *Engyodontium* (Figs 4, S4), which is monophyletic, while *Lecanicillium* was considered to be polyphyletic (Sung *et al.* 2007, Kepler *et al.* 2017), leading to the description of several new genera including *Corniculantispora*, *Corpulentispora*, *Zarea* and *Zouia* (Khonsanit *et al.* 2024). The placement of *E. huhutii* is supported in 100 % of the bootstraps and with a posterior probability of 1.00. In addition, the microscopic pictures provided by Zhou *et al.* (2022) showed the production of denticulate conidiogenous cells by *E. huhutii*; this is a distinctive feature of *Engyodontium*. Khonsanit *et al.* (2024) already considered *L. huhutii* as an *Engyodontium* species, but without formally transferring this species into the genus. We consider that the phylogenetic and morphologic features are relevant enough to justify transferring this species to *Engyodontium*.

Engyodontium latronense J. Leplat, ***sp. nov.*** MB 850837. Fig. 11.
Etymology: The epithet *latronense* refers to the name of the cave from which the type strain was isolated, *i.e.* Baume Latrone cave.

GenBank: OR264331 (ITS), OR263662 (nrLSU), OR269660 (*rpb1*), OR291093 (*rpb2*), OR291131 (*tef-1α*).

Typus: **France**, Sainte-Anastasie, 43°55’49”N, 4°20’04”E, Jul. 2021, isolated from air sampling in the Baume Latrone cave, collected and isolated by the microbiologists of the French Historical Monuments Research Laboratory (**holotype** CBS 150569, preserved in a metabolically inactive state), culture ex-type CBS 150569 = LRMH C469.

Known distribution: France, Occitanie region.

Description: *Colonies* on MEA reached 20–23 mm diam. at 25 °C, white, velutinous, radially striate. Reverse brownish orange. No growth at 30 °C. Colonies on PDA reached 20–24 mm diam. after 10 d at 25 °C, white, velutinous, radially striate. Reverse light yellow. No growth at 30 °C. *Hyphae* septate, smooth walled, hyaline. *Conidiogenous cells* arising laterally or terminally from prostrate hyphae, solitary or in whorls of 2–3, straight or slightly curved, tapering to the apex, polyblastic, bearing thin, perpendicular denticles scattered along the upper half, 11–31 × 1.1–1.3 um. *Conidia* aseptate, hyaline, smooth-walled, ellipsoidal to cylindrical with a rounded end, 2.8–6.0 × 1.4–1.8 µm.

Notes: *Engyodontium parvisporum* and *E. huhutii* are phylogenetically the closest species to *E. latronense* (Fig. 4). *Engyodontium latronense* can be distinguished from these two species by its production of larger conidiogenous cells and larger conidia (de Hoog 1978, Zhou *et al.* 2022). The two former species do not seem to produce the large cylindrical conidia recovered in *E. latronense*. The microscopic features of *E. latronense* seem closer to those expressed by *E. recidentatum*, which vary according to the strain examined (Gams *et al.* 1984). The perpendicular denticles and the size of conidia expressed by *E. latronense* correspond to those expressed by some *E. rectidentatum* strains, and in particular *E. recidentatum* CBS 641.74. This strain was used as a reference in this study and was found to be phylogenetically different from *E. latronense*. These two species are differentiated by twenty base pairs concerning only ITS, nrLSU and *tef-1α* regions since no sequence is available for *rpb1* and *rpb2* regions for *E. recidentatum* CBS 641.74.

Frescium J. Leplat, ***gen. nov.*** MB 850838.

Etymology: The name of the genus refers to the support from which the two species of this new genus were isolated, *i.e.* a fresco in the crypt of Saint-Savin-sur-Gartempe Abbey church.

Description: *Hyphae* septate, smooth-walled, hyaline. *Conidiogenous cells* arising laterally or terminally from prostrate hyphae, solitary or in whorls of 2–3, straight, monoblastic or polyblastic. *Conidia* aseptate, hyaline, smooth-walled, cylindrical to ellipsoidal.

Type species: *Frescium savinense* J. Leplat

Notes: This genus was established to accommodate two unknown species recovered from the Saint-Savin crypt fresco in a previous study (Leplat *et al*. 2017). These two species were phylogenetically related (Figs 8, S1), but clearly distinct for both molecular and morphological features. The genus clearly belongs to *Hypocreales* but cannot be easily placed in any known family, with the closest correspondences being found in *Clavicipitaceae*, *Cordycipitaceae*, *Hypocreaceae*, *Nectriaceae*, *Ophicordycipitaceae* or *Valsonectriaceae* depending on the DNA locus considered. *Neobaryopsis*, currently composed of the single species *N. andesis*, is the closest from *Frescium* phylogenetically (Fig. 8). The two genera are relatively distant since they are differentiated by 50 bp when considering only ITS and nrLSU regions, no sequence being available for *rpb1*, *rpb2* and *tef-1α* regions

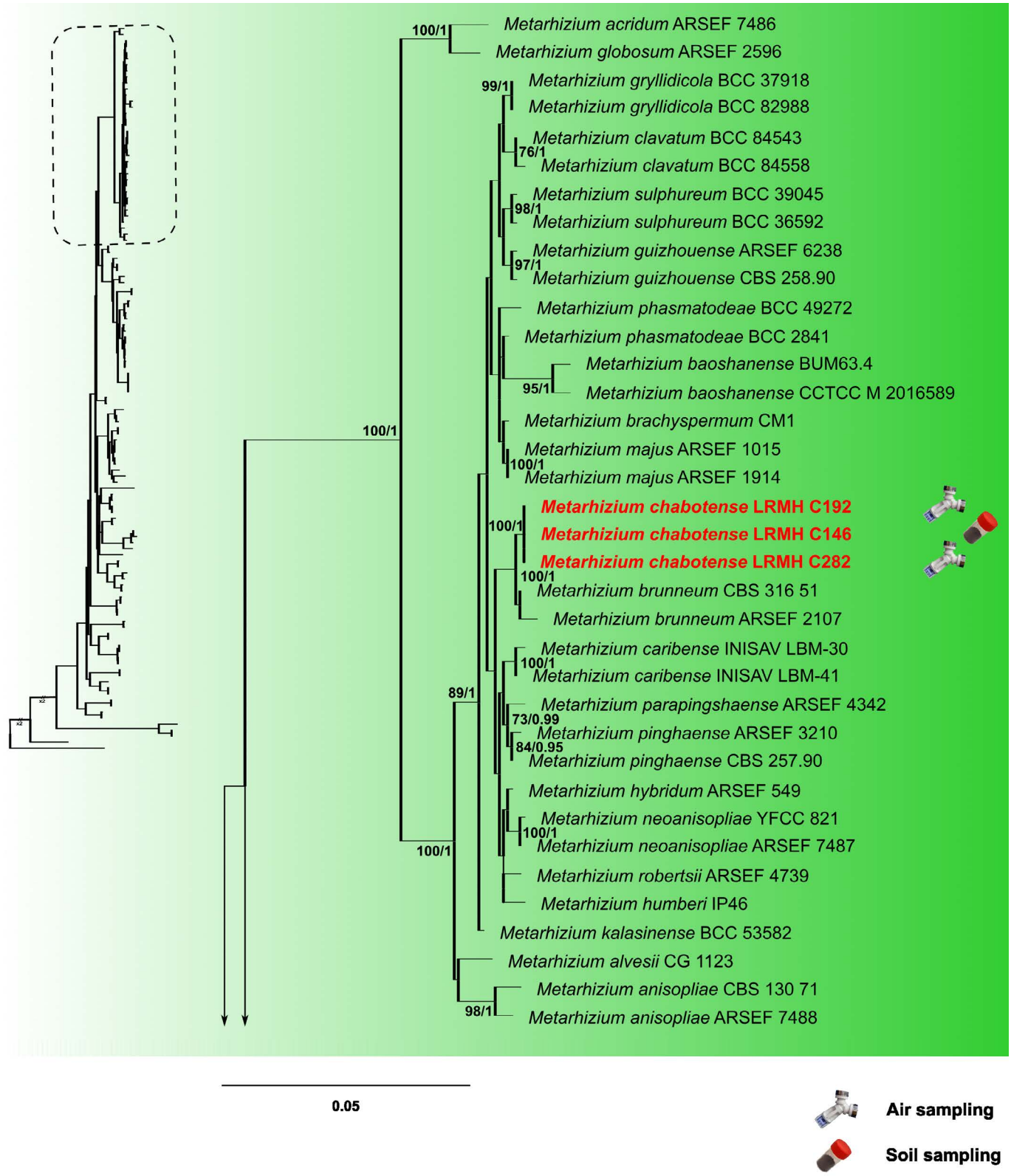

Fig. 7. Phylogenetic studies through maximum likelihood (ML) and Bayesian inference (BI) among *Metarhizium* species. The trees were rooted with *Torrubiella ratticaudata* ARSEF 1915 (*Clavicipitaceae*) as an outgroup. Bootstrap values greater than or equal to 70 % and Bayesian posterior probabilities greater than or equal to 0.70 are located close to the corresponding nodes. The newly described species from studied strains are displayed in bold red print.

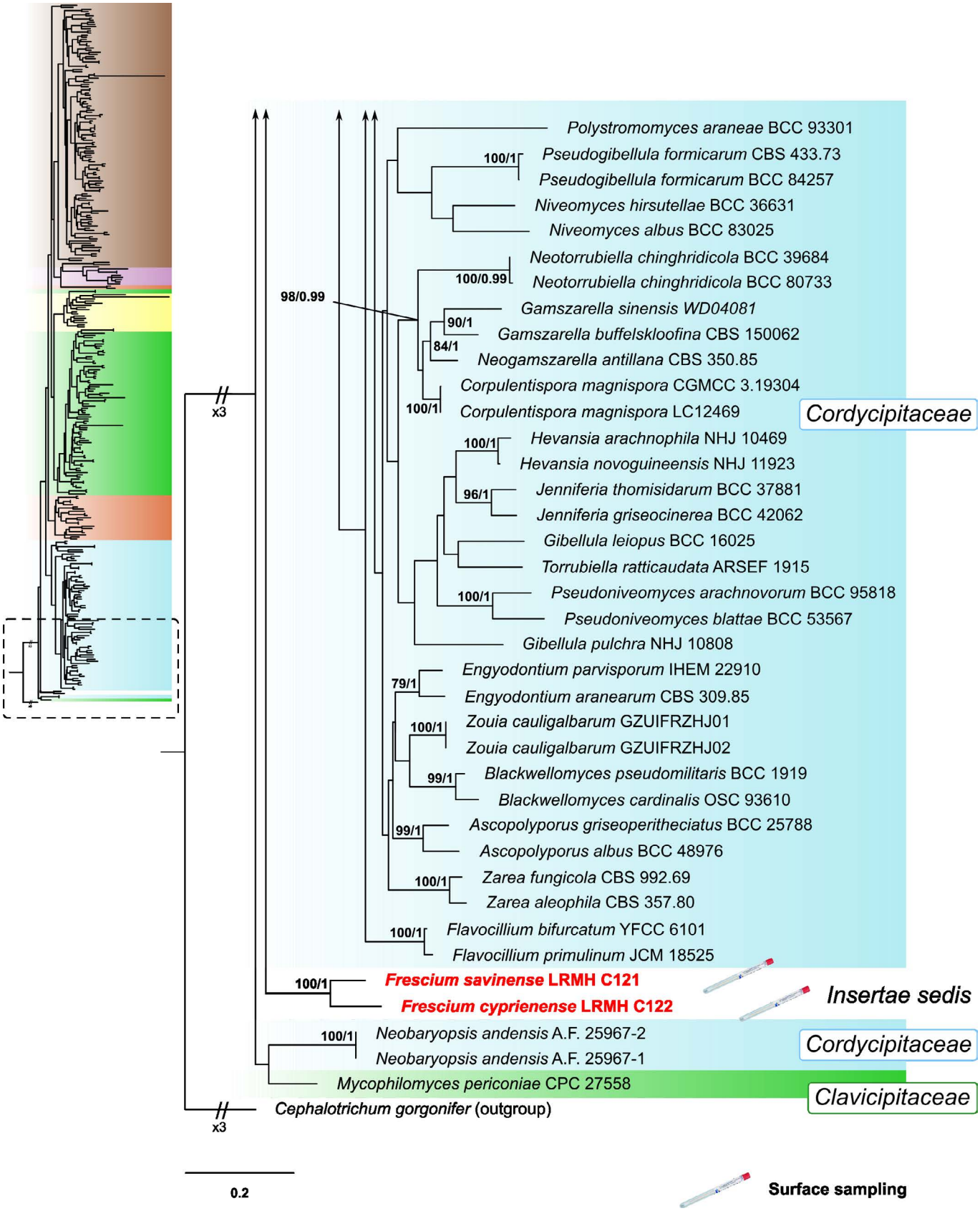

Fig. 8. Phylogenetic studies through maximum likelihood (ML) and Bayesian inference (BI) of the strains LRMH C121 and LRMH C122 among the closest *Hypocreales* families determined by the study of single DNA loci. The trees were rooted with *Cephalotrichum gorgonifer* (*Microascales*; accession number ONZQ00000000) as an outgroup. Bootstrap values greater than or equal to 70 % and Bayesian posterior probabilities greater than or equal to 0.70 are located close to the corresponding nodes. Newly described species from studied strains are displayed in bold red print.

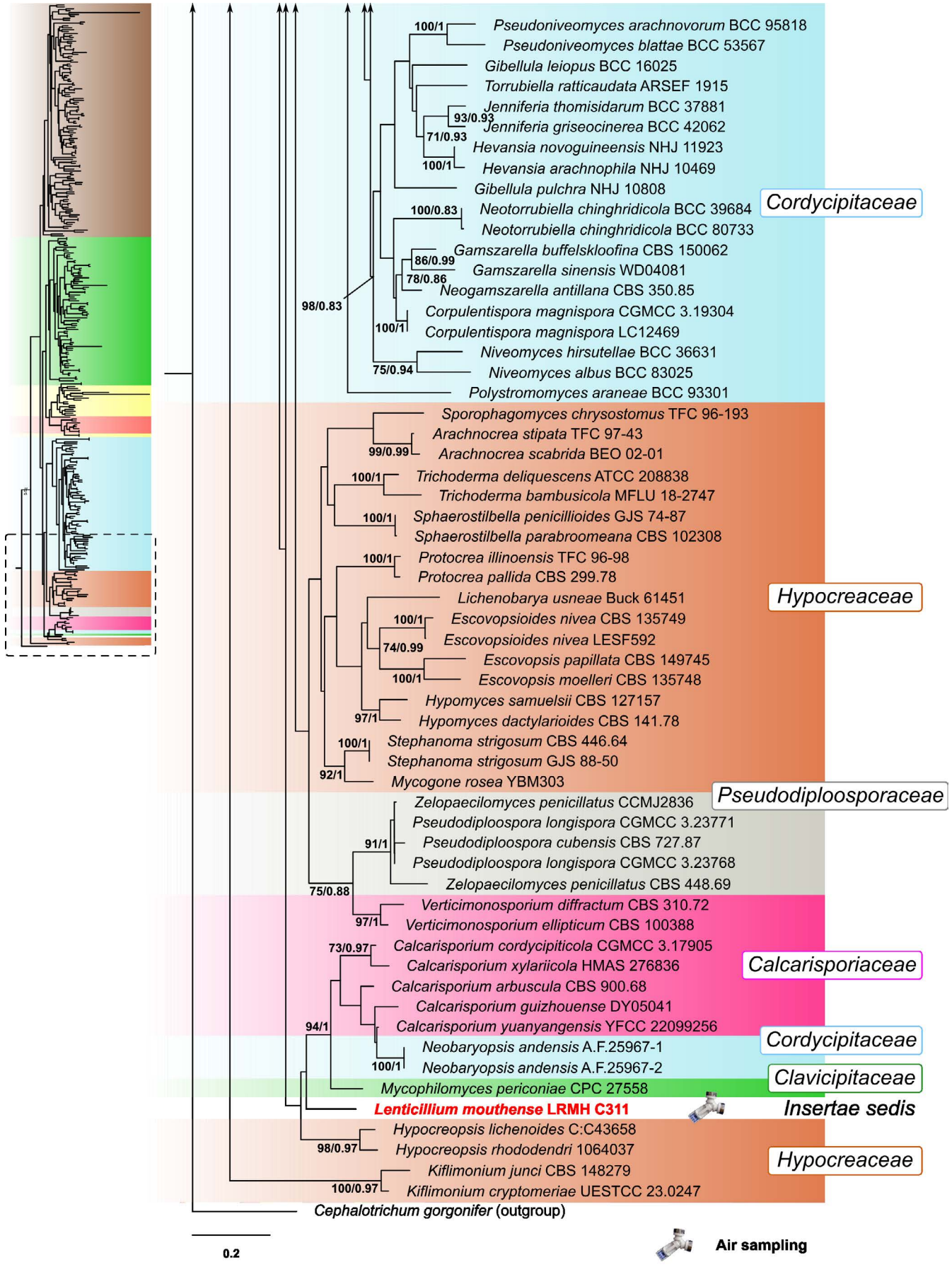

Fig. 9. Phylogenetic studies through maximum likelihood (ML) and Bayesian inference (BI) of the strain LRMH C311 among the closest *Hypocreales* families determined by the study of single DNA loci. The trees were rooted with *Cephalotrichum gorgonifer* (*Microascales*; accession number ONZQ00000000) as an outgroup. Bootstrap values greater than or equal to 70 % and Bayesian posterior probabilities greater than or equal to 0.70 are located close to the corresponding nodes. The newly described species from studied strains is displayed in bold red print.

Fig. 10. Morphological features of *Corniculantispora pseudoaranearum*. **A, B.** Upper views of the culture on MEA and PDA (10 d at 25 °C). **C, D.** Reverse views of the culture on MEA and PDA (10 d at 25 °C). **E, F.** Conidiogenous cells and conidia. Scale bars: E–F = 10 µm.

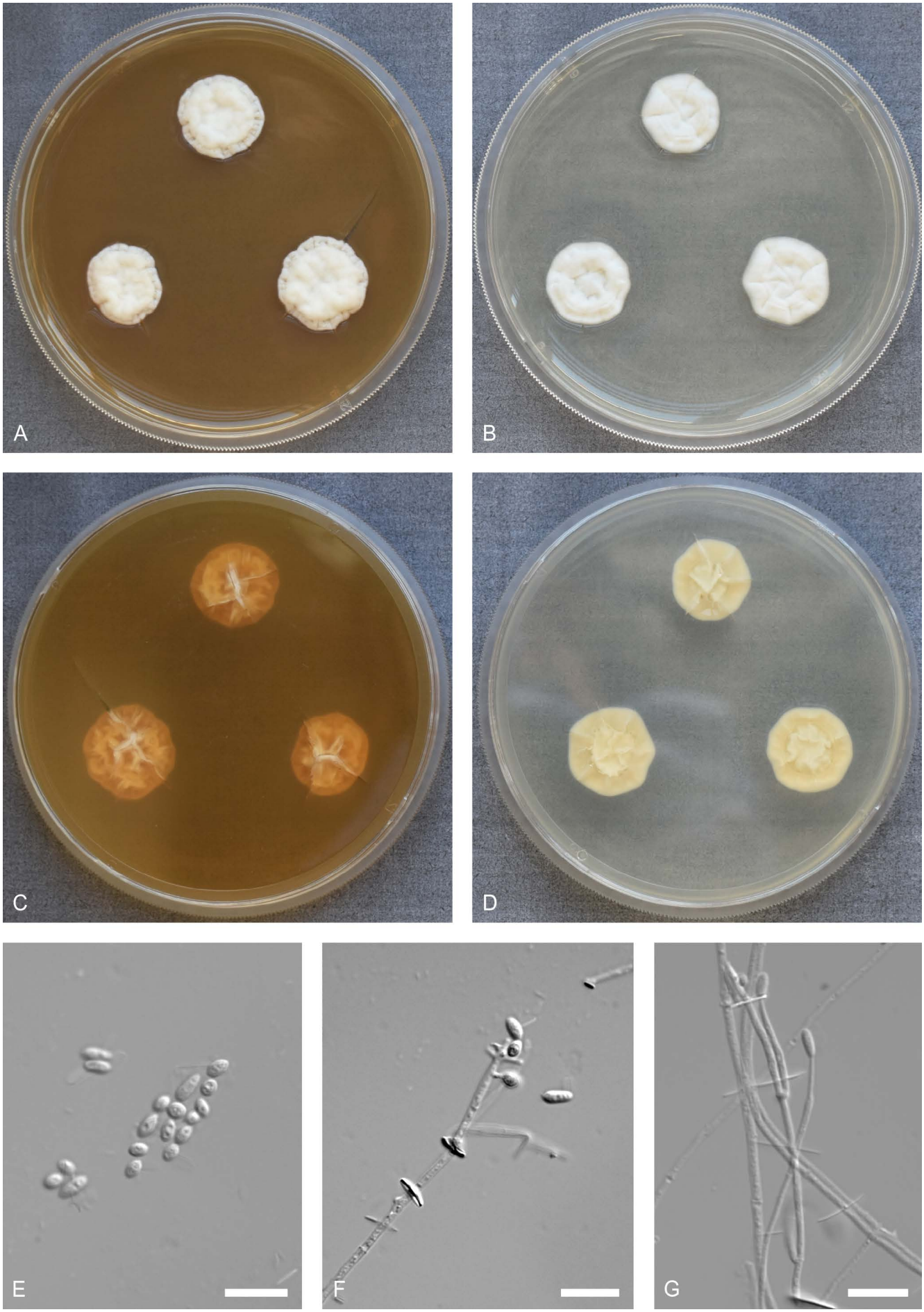

Fig. 11. Morphological features of *Engyodontium latronense*. **A, B.** Upper views of the culture on MEA and PDA (10 d at 25 °C). **C, D.** Reverse views of the culture on MEA and PDA (10 d at 25 °C). **E–G.** Conidiogenous cells and conidia. The pictures display the typical conidial growth from perpendicular denticles on conidiogenous cells and the various shapes of conidia. Scale bars: E–G = 10 µm.

of *N. andesis*. *Frescium* includes species with conidiogenous cells of different shapes, since monoblastic and polyblastic cells were observed. This kind of polyblastic cell has already been observed in several *Hypocreales* families, such as *Calacarisporiaceae* or in *Cordycipitaceae* (Sun *et al*. 2017, Araújo *et al.* 2022, Colmán *et al.* 2025).

Frescium cyprienense J. Leplat, ***sp. nov.*** MB 850839. Fig. 12.

Etymology: The epithet *cyprienense* refers to the name of the mural painting from which the species was isolated, *i.e.* "The martyr of Saint-Savin and Saint-Cyprien".

GenBank: KX821730 (ITS), OR263630 (nrLSU), OR269628 (*rpb1*), OR291062 (*rpb2*), OR291101 (*tef-1α*).

Typus: **France**, Saint-Savin-sur-Gartempe 46°34'01"N, 0°51'52"E, Nov. 2015, isolated from a surface sampling on the wall paintings of the Saint-Savin-sur-Gartempe Abbey church crypt, collected and isolated by the microbiologists of the French Historical Monuments Research Laboratory (**holotype** CBS 150562, preserved in a metabolically inactive state), culture ex-type CBS 150562 = LRMH C122.

Known distribution: France, Nouvelle-Aquitaine region.

Description: *Colonies* on MEA reached 17–20 mm diam. at 25 °C, white, velutinous, radially striate. Reverse light orange. Traces of growth after 10 d at 30 °C. Colonies on PDA reached 15–18 mm diam. at 25 °C, white, velutinous. Reverse white. Traces of growth at 30 °C. *Hyphae* septate, smooth-walled, hyaline. *Conidiogenous cells* arising laterally or terminally from prostrate hyphae, mainly solitary, or in whorls of 2–3, straight, gradually tapering to the apex, 15.2–20.4 × 1–1.5 µm. *Conidia* aseptate, hyaline, smooth walled, solitary, cylindrical, ellipsoidal or fusiform 2.5–5 × 1.2–1.6 µm.

Notes: The genus *Frescium* was described to accommodate two phylogenetically related but distinct species (Figs 8, S1). *Frescium cyprienense* can be distinguished from *F. savinense* by a slower growth rate on PDA at 25 °C and a growth limited to just traces of growth on PDA at 30 °C, while substantial growth was noted in *F. savinense*. In addition, conidiogenous cells produced by *F. cyprienense* are longer than those produced by *F. savinense*. The conidiogenous cell produced by *F. cyprienense* are monoblastic, while *F. savinense* produced polyblastic conidiogenous cells. The two species are relatively distant phylogenetically since 235 bp differentiate this two species when considering the concatenation of ITS, nrLSU, *rpb1*, *rpb2* and *tef-1α* sequences.

Frescium savinense J. Leplat, ***sp. nov.*** MB850840. Fig. 13.

Etymology: The epithet *savinense* refers to the name of the mural painting from which the species was isolated, *i.e.* "The martyr of Saint-Savin and Saint-Cyprien".

GenBank: KX821729 (ITS), OR263629 (nrLSU), OR269627 (*rpb1*), OR291061 (*rpb2*), OR291100 (*tef-1α*).

Typus: **France**, Saint-Savin-sur-Gartempe 46°34'01"N, 0°51'52"E, Nov. 2015, isolated from a surface sampling on the wall paintings of the Saint-Savin-sur-Gartempe Abbey church crypt, collected and isolated by the microbiologists of the French Historical Monuments Research Laboratory (**holotype** CBS 150561, preserved in a metabolically inactive state), culture ex-type CBS 150561 = LRMH C121.

Known distribution: France, Nouvelle-Aquitaine region.

Description: Colonies on MEA reached 18–20 mm diam. at 25 °C, white, velutinous, slightly radially striate. Reverse orange. No growth at 30 °C. Colonies on PDA reached 21–22(–28) mm diam. at 25 °C, white to yellowish white, velutinous. Reverse light yellow. Colonies reached 12–15 mm diam. at 30 °C. *Hyphae* septate, smooth-walled, hyaline. *Conidiogenous cells* arising laterally or terminally from prostrate hyphae, solitary or in whorls of 2–3, straight, polyblastic, 6.8–14 × 0.8–1.2 µm. *Conidia* aseptate, hyaline, smooth walled, cylindrical to ellipsoidal 3–4 × 1–1.4 µm.

Notes: The genus *Frescium* was described to accommodate two phylogenetically related but distinct species (Figs 8, S1). *Frescium savinense* can be distinguished from *F. cyprienense* by a faster growth rate on PDA at 25 °C and by a substantial growth on PDA at 30 °C, while only traces of growth were noted in *F. cyprienense*. In addition, conidiogenous cells produced by *F. savinense* are smaller than those produced by *F. cyprienense*. The conidiogenous cells produced by *F. savinense* are polyblastic, while *F. cyprienense* produced monoblastic conidiogenous cells. The two species are relatively distant phylogenetically since 235 bp differentiate the two species when considering the concatenation of ITS, nrLSU, *rpb1*, *rpb2* and *tef-1α* sequences.

Gamszarea americana (M.M. Teixeira *et al.*) J. Leplat, ***comb. nov.*** MB 849571.
Basionym: *Parengyodontium americanum* M.M. Teixeira *et al.*, *Fungal Genetics and Biology* **138**: 8. 2020.

Typus: **USA**, Arizona, patient with pulmonary infection, initially diagnosed with coccidioidomycosis, *M. Teixeira et al*., **holotype** CBS 144514 (preserved in a metabolically inactive state).

Description and illustration: See Teixeira *et al*. (2020).

Known distribution: United States of America.

Notes: *Gamszarea americana* was first described as a *Parengyodontium* species despite the authors having noted that the microscopic features of this species correspond more to *Lecanicillium* (Teixeira *et al*. 2020). More specifically, the species does not display the typical zigzag shape of the phialides neck observed in other *Parengyodontium* species. The verticillate conidiophores bear phialides that are solitary or in whorls of two, which corresponds to *Gamszarea* features. The phylogenetic studies confirmed the place of *G. americana*, which is placed on a clade among *Gamszarea* species supported by 100 % of bootstraps and with a posterior probability of 1.00 (Fig. S4). The closest species from *Gamszarea americana* is *G. testudinea*. The clade composed of these two species is supported by 100 % of bootstraps and with a posterior probability of 1.00

(Fig. 5). The microscopic features of these two species seem close, expressing conidiophores with irregular branches bearing solitary phialides or in whorls of 2–4 (Crous *et al.* 2018, Teixeira *et al.* 2020). However, the production of macroconidia was noted in *G. testudinea* and not in *G. americana*.

Gamszarea cavernicola J. Leplat, ***sp. nov.*** MB 850841. Fig. 14.

Etymology: The epithet *cavernicola* refers to the environment where the three strains of this species were recovered, *i.e.* a Paleolithic decorated cave.

GenBank: OR264321 (ITS), OR263656 (nrLSU), OR269654 (*rpb1*), OR291087 (*rpb2*), OR291125 (*tef-1α*).

Typus: **France**, Vallon-Pont-d'Arc, 44°23'17"N, 4°24'58"E, Jan. 2019, isolated from surface sampling on the wall of Chauvet cave, collected and isolated by the microbiologists of the French Historical Monuments Research Laboratory (**holotype** CBS 150567, preserved in a metabolically inactive state), culture ex-type CBS 150567 = LRMH C326.

Known distribution: France, Auvergne-Rhône-Alpes and Nouvelle-Aquitaine regions.

Description: *Colonies* on MEA reached 29–34 mm diam. at 25 °C, white, velutinous, radially striate. Reverse brownish orange. Colonies reached 4–6 mm diam. at 30 °C. Colonies on PDA reached 28–33 mm diam. at 25 °C, white, velutinous, radially striate. Reverse light yellow to greyish yellow. Colonies reached 13–17 mm diam. at 30 °C. *Hyphae* septate, smooth-walled, hyaline. *Conidiophores* arising laterally from prostrate hyphae. *Conidiogenous cells* arising were solitary or in whorls of 2, straight or slightly curved, tapering to the apex, 15–23 × 0.9–1.5 µm. *Conidia* aggregated in slimy heads, aseptate, hyaline, smooth-walled, dimorphic, microconidia ellipsoidal to fusiform, sometimes curved, 2.6–3.0 × 1.2–1.8 µm, macroconidia fusiform, sometimes asymmetrically curved, 4.0–5.9 × 0.9–1.4 µm.

Notes: *Gamszarea microspora* and *G. gracilis* are the closest species to *G. cavernicola* based both on phylogenetic and morphologic features. The clade composed of these three species is supported by 91 % of bootstraps and with a posterior probability of 1.00 (Fig. 5). The three species have also very similar microscopic characteristics, making it difficult to make a distinction between them based on these characteristics. In addition, the three species were isolated from comparable supports: the types of *G. cavernicola* and *G. microspora* were isolated through surface samplings on the rock of a cave, and *G. gracilis* was isolated through surface sampling on limestone in a church (Ponizovskaya *et al.* 2020, Zhang *et al.* 2020). These three species can be differentiated based on phylogenetic features. *Gamszarea microspora* strains are gathered on a clade supported in 99 % of the bootstraps and with a posterior probability of 1.00 (Fig. 5). Fifty-four bp differentiate *G. cavernicola* from *G. microspora* clade when considering ITS, nrLSU, *rpb2* and *tef-1α* sequences, no sequence being available for *G. microspora rpb1* region. Only ITS and *tef-1α* sequences are available for *G. gracilis*, resulting in eleven different base pairs from *G. cavernicola*.

Other strains examined: **France**, LRMH C231, Marquay 44°56'44"N, 1°05'49"E, Oct. 2016, isolated from surface sampling in Cap Blanc shelter, collected and isolated by the microbiologists of the French Historical Monuments Research Laboratory; LRMH C246, Prignac-et-Marcamps 45°02'20"N, 0°30'06"O, Oct. 2016, isolated from air sampling in Pair-non-Pair cave, collected and isolated by the microbiologists of the French Historical Monuments Research Laboratory.

Gamszarea gracilis (Ponizovskaya *et al.*) J. Leplat, ***comb. nov.*** MB 849572.
Basionym: *Lecanicillium gracile* Ponizovskaya *et al.*, *Phytotaxa* **443**: 268. 2020.

Typus: **Russia**, Vladimir region, Kideksha village, Church of Boris and Gleb (XII century), wall area with high moisture content and precipitation of salts at the surface, loose limestone, 13 Jun. 2013, *V.B. Ponizovskaya & N.L. Rebrikova* (**holotype** CBS H-23932, ex-type culture CBS 142821).

Description and illustration: See Ponizovskaya *et al.* (2020).

Known distribution: Russia, Vladimir region: Kideksha village, Church of Boris and Gleb (XII century).

Notes: *Gamszarea gracilis* was first described as a *Lecanicillium* species, like many other species in the *Gamszarea* (Zhang et al. 2020). The microscopic features of *G. gracilis* correspond to those observed in *Gamszarea*, i.e. phialides that are solitary or in whorls, and produce both microconidia and macroconidia in heads (Ponizovskaya *et al.* 2020). The phylogenetic studies confirmed the place of *G. gracilis*, which is placed on a clade among *Gamszarea* species supported by 99 % of bootstraps and with a posterior probability of 1.00 (Fig. S4). *Gamszarea microspora* and *G. cavernicola* are the closest species to *G. gracilis*. The clade composed of these three species is supported by 91 % of bootstraps and with a posterior probability of one (Fig. 5). The three species seem to have very similar morphological features, making it difficult to differentiate between them based on these characteristics. In addition, the three species were isolated from comparable supports: type specimens were isolated through surface sampling on limestone in a church or on the rock of caves. Several authors already proposed *L. gracile* as a *Gamszarea* species (Zhou *et al*. 2022, Khonsanit *et al.* 2024), but without formally transferring this species into the genus. We consider that phylogenetic and morphologic features are relevant enough to justify moving this species to *Gamszarea* genus.

Lenticillium J. Leplat, ***gen. nov.*** MB 850843.

Etymology: The name of the genus refers to the slow growth rate of the type species, "lent" meaning "slow" in French.

Description: *Hyphae* septate, smooth-walled, hyaline. *Conidiogenous cells* arising laterally from prostrate hyphae, solitary, occasionally in whorls of 2, straight. *Conidia* aseptate, hyaline, smooth walled, cylindrical, ellipsoidal or fusiform.

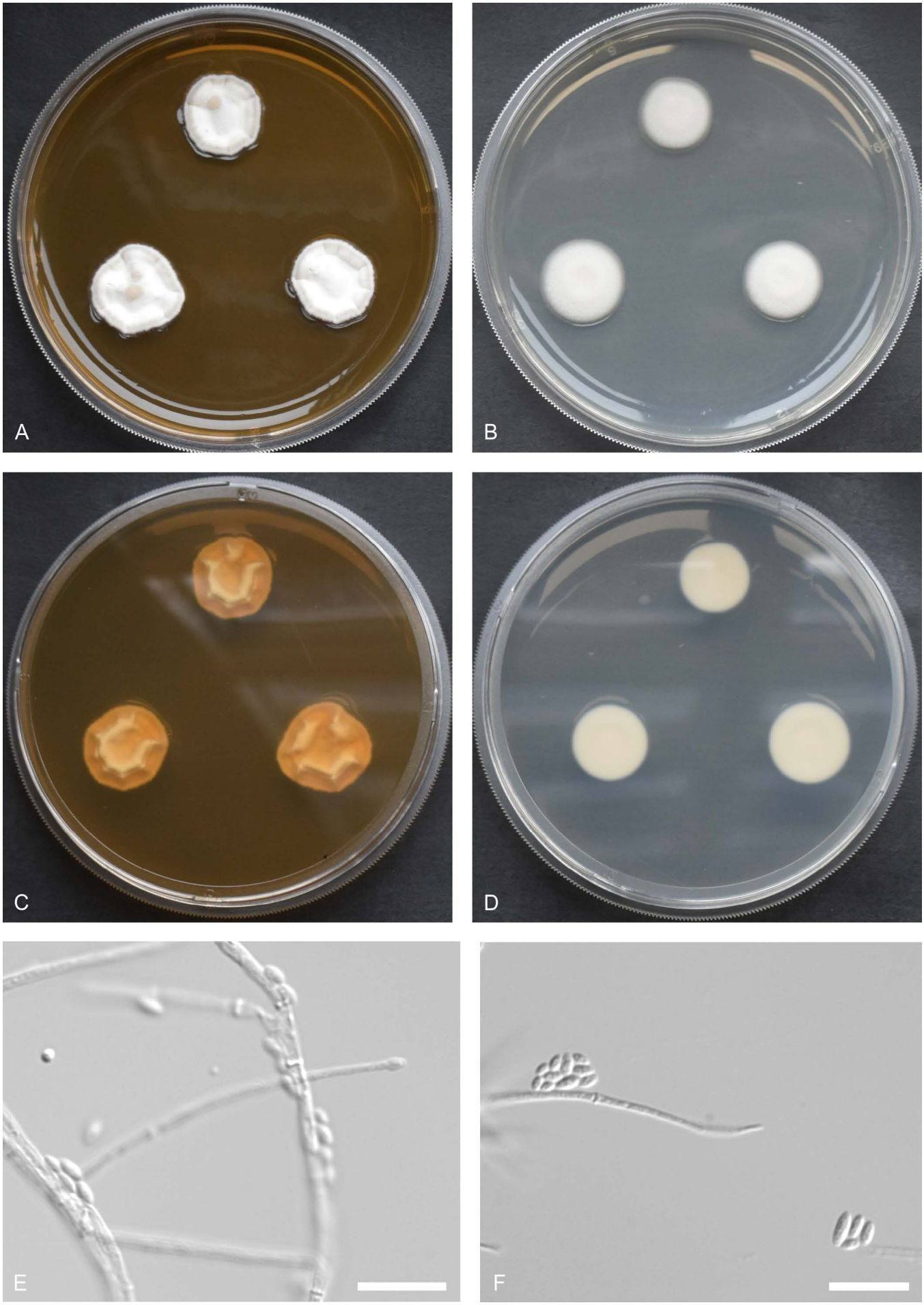

Fig. 12. Morphological features of *Frescium cyprienense*. **A, B.** Upper views of the culture on MEA and PDA (10 d at 25 °C). **C, D.** Reverse views of the culture on MEA and PDA (10 d at 25 °C). **E, F.** Conidiogenous cells and conidia of various shapes. Scale bars: E–F = 10 µm.

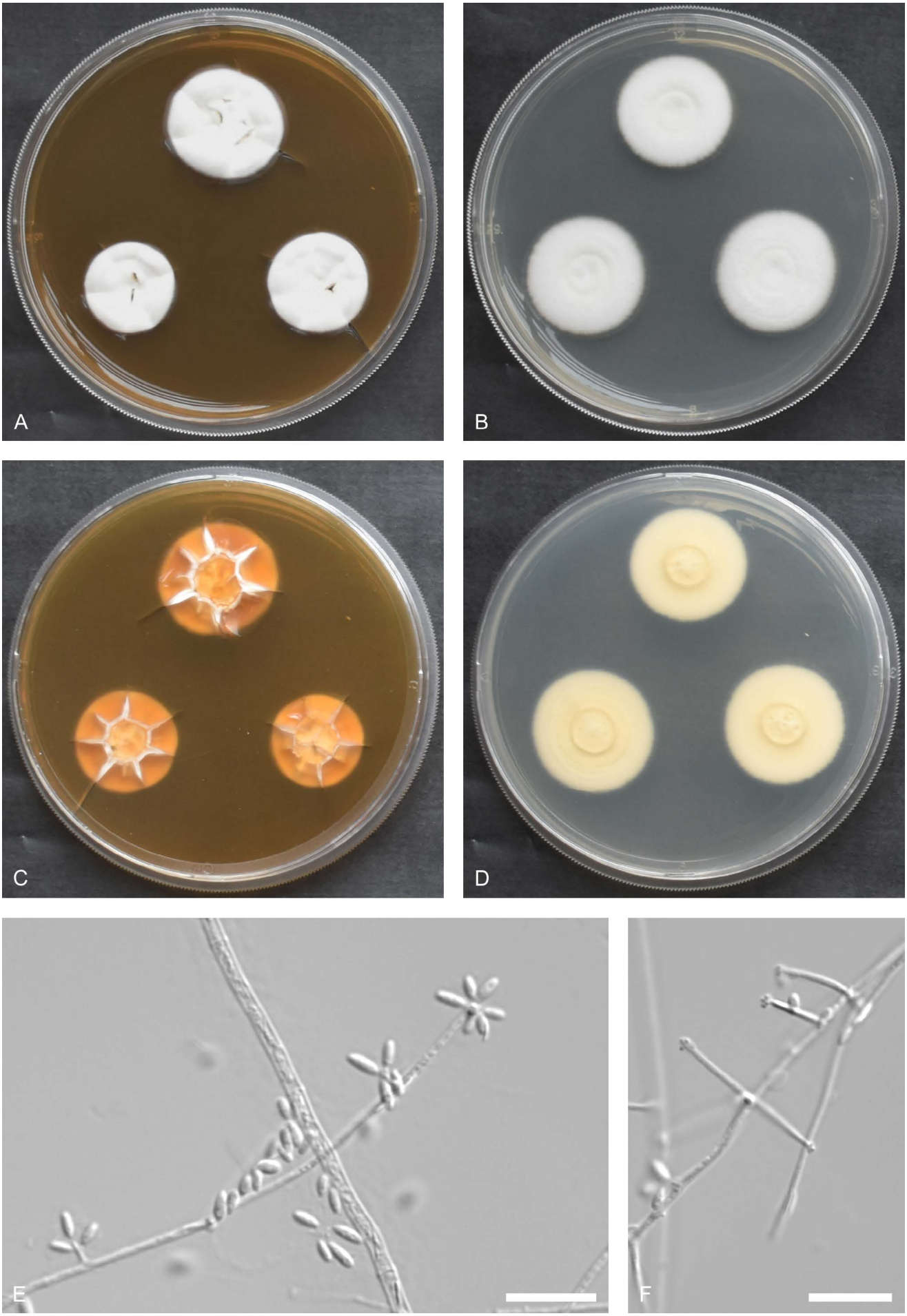

Fig. 13. Morphological features of *Frescium savinense*. **A, B.** Upper views of the culture on MEA and PDA (10 d at 25 °C). **C, D.** Reverse views of the culture on MEA and PDA (10 d at 25 °C). **E, F.** Polyblastic conidiogenous cells and conidia. Scale bars: E–F = 10 µm.

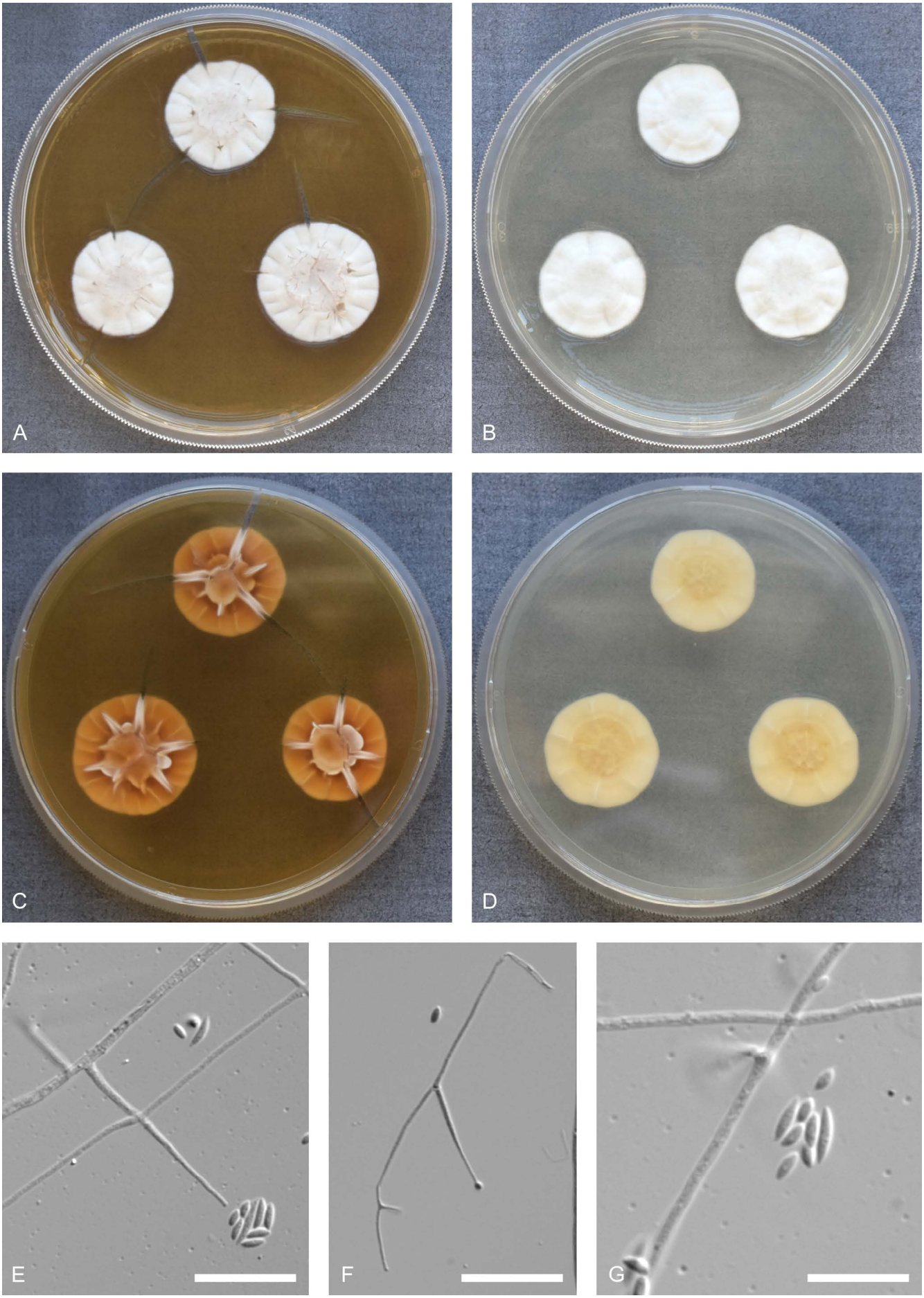

Fig. 14. Morphological features of *Gamszarea cavernicola*. **A, B.** Upper views of the culture on MEA and PDA (10 d at 25 °C). **C, D.** Reverse views of the culture on MEA and PDA (10 d at 25 °C). **E, F.** Conidiogenous cells and conidia aggregated in slimy heads. G. Macroconidia and microconidia. Scale bars: E–G = 10 µm.

Type species: *Lenticillium mouthense* J. Leplat

Notes: *Lenticillium* clearly belongs to *Hypocreales* but cannot be easily placed in any known family, with the closest correspondences being found in *Calcarisporiaceae*, *Clavicipitaceae, Cordycipitaceae, Hypocreaceae, Nectriaceae*, *Ophicordycipitaceae, Polycephalomycetaceae or Pseudodiploosporaceae* depending on the DNA locus considered (Figs 9, S1). The phylogenetically closest genera are *Hypocreopsis* and *Mycophilomyces*, represented by the single species *M. periconiae*. The comparison with *Lenticillium* was only based on ITS sequences for *Hypocreopsis* and on ITS and nrLSU sequences for *Mycophilomyces* resulting in 18 and 38 different bp respectively.

Lenticillium mouthense J. Leplat, ***sp. nov.*** MB 850848. Fig. 15.

Etymology: The epithet *mouthense* refers to the name of the cave from which the species was isolated, *i.e.* La Mouthe cave.

GenBank: OR264319 (ITS), OR263654 (nrLSU), OR269652 (*rpb1*), OR291085 (*rpb2*), OR291123 (*tef-1α*).

Typus: **France**, Les Eyzies-de-Taillac-Sireuil, 44°55'29"N, 1°01'14"E, Oct. 2018, isolated from air sampling in La Mouthe cave, collected and isolated by the microbiologists of the French Historical Monuments Research Laboratory (**holotype** CBS 150566, preserved in a metabolically inactive state), culture ex-type CBS 150566 = LRMH C311.

Known distribution: France, Nouvelle-Aquitaine region.

Description: *Colonies* on MEA reached 16–19 mm diam. at 25 °C, white, velutinous, slightly radially striate. Reverse brownish orange to light brown. No growth at 30 °C. Colonies on PDA reached 18–20 mm diam. at 25 °C, white, velutinous. Reverse white to light yellow. No growth at 30 °C. *Hyphae* septate, smooth-walled, hyaline. *Conidiogenous cells* arising laterally from prostrate hyphae, mostly solitary, occasionally in whorls of 2, straight, 9.5–12.5 × 1.5–1.6 µm. *Conidia* aseptate, hyaline, smooth-walled, cylindrical, ellipsoidal or fusiform, 1.9–5.2 × 1.6–2.0 µm.

Note: See the description of *Lenticillium*.

Metarhizium chabotense J. Leplat, ***sp. nov.*** MB 850849. Fig. 16.

Etymology: The epithet *chabotense* refers to the name of the cave from which the three specimens of the species were isolated, *i.e.* Chabot cave.

GenBank: OR264312 (ITS), OR263647 (nrLSU), OR269645 (*rpb1*), OR291078 (*rpb2*), OR291116 (*tef-1α*).

Typus: **France**, Aiguèze 44°19'22"N, 4°32'28"E, May 2017, isolated from air sampling in Chabot cave, collected and isolated by the microbiologists of the French Historical Monuments Research Laboratory (**holotype** CBS 150565, preserved in a metabolically inactive state), culture ex-type CBS 150565 = LRMH C282.

Known distribution: France, Occitanie region.

Description: *Colonies* on MEA reached 40–42 mm diam. at 25 °C, white to pale yellow dotted with olive, floccose. Reverse brownish orange to light brown. Colonies reached 40–42 mm diam. at 30 °C. Colonies on PDA reached 32–35 mm diam. at 25 °C, greyish yellow dotted with olive, velvety to floccose. Reverse brownish orange to light brown. Colonies reached 41–45 mm diam. at 30 °C. *Hyphae* septate, hyaline and smooth walled. *Conidiogenous cells* arranged in candelabrum-like dense whorls of branches, cylindrical, sometimes with an expanded median part, 9.8–13 × 1.7–3.8 µm, tapering into a short neck. *Conidia* arranged in long chains, cylindrical, one celled, 6.2–7.8 × 2.2–2.5 µm.

Notes: *Metarhizium chabotense* seems to be very close to *M. brunneum*, in both morphological and molecular terms. Incidentally, it is practically impossible to distinguish between the members of the *M. anisopliae* complex based on microscopic features alone (Bischoff *et al*. 2009). The particular shape of some conidiogenous cells of *M. chabotense*, namely with an expanding medium part, does not seem to have been described in *M. brunneum*. The phylogenetic study supports the distinction between the two species. *Metarhizium chabotense* strains form a clade distinct from *M. brunneum* clade (Fig. 7). The *M. chabotense* clade is supported in 100 % of the bootstraps and with a posterior probability of 1.00. *Metarhizium chabotense* and *M. brunneum* clades are the result of eighteen different base pairs when considering the concatenation of ITS, nrLSU, *rpb1*, *rpb2* and *tef-1α* sequences.

Other strains examined: **France**, LRMH C146, Aiguèze 44°19'22"N, 4°32'28"E, Sep. 2015, isolated from soil sampling in Chabot cave, collected and isolated by the microbiologists of the French Historical Monuments Research Laboratory; LRMH C192, Aiguèze 44°19'22"N, 4°32'28"E, Jun. 2016, isolated from air sampling in Chabot cave, collected and isolated by the microbiologists of the French Historical Monuments Research Laboratory.

Simplicillium aquitainense J. Leplat, ***sp. nov.*** MB 850850. Fig. 17.

Etymology: The epithet *aquitainense* refers to the name of the region where the holotype of the species was isolated, *i.e.* Nouvelle-Aquitaine region.

GenBank: OR264317 (ITS), OR263652 (nrLSU), OR269650 (*rpb1*), OR291083 (*rpb2*), OR291121 (*tef-1α*).

Typus: **France**, Prignac-et-Marcamps, 45°02'20"N, 0°30'06"O, Oct. 2018, isolated from surface sampling in Pair-non-Pair cave, collected and isolated by the microbiologists of the French Historical Monuments Research Laboratory (**holotype** CBS 150708, preserved in a metabolically inactive state), culture ex-type CBS 150708 = LRMH C300.

Known distribution: France, Nouvelle-Aquitaine and Occitanie regions.

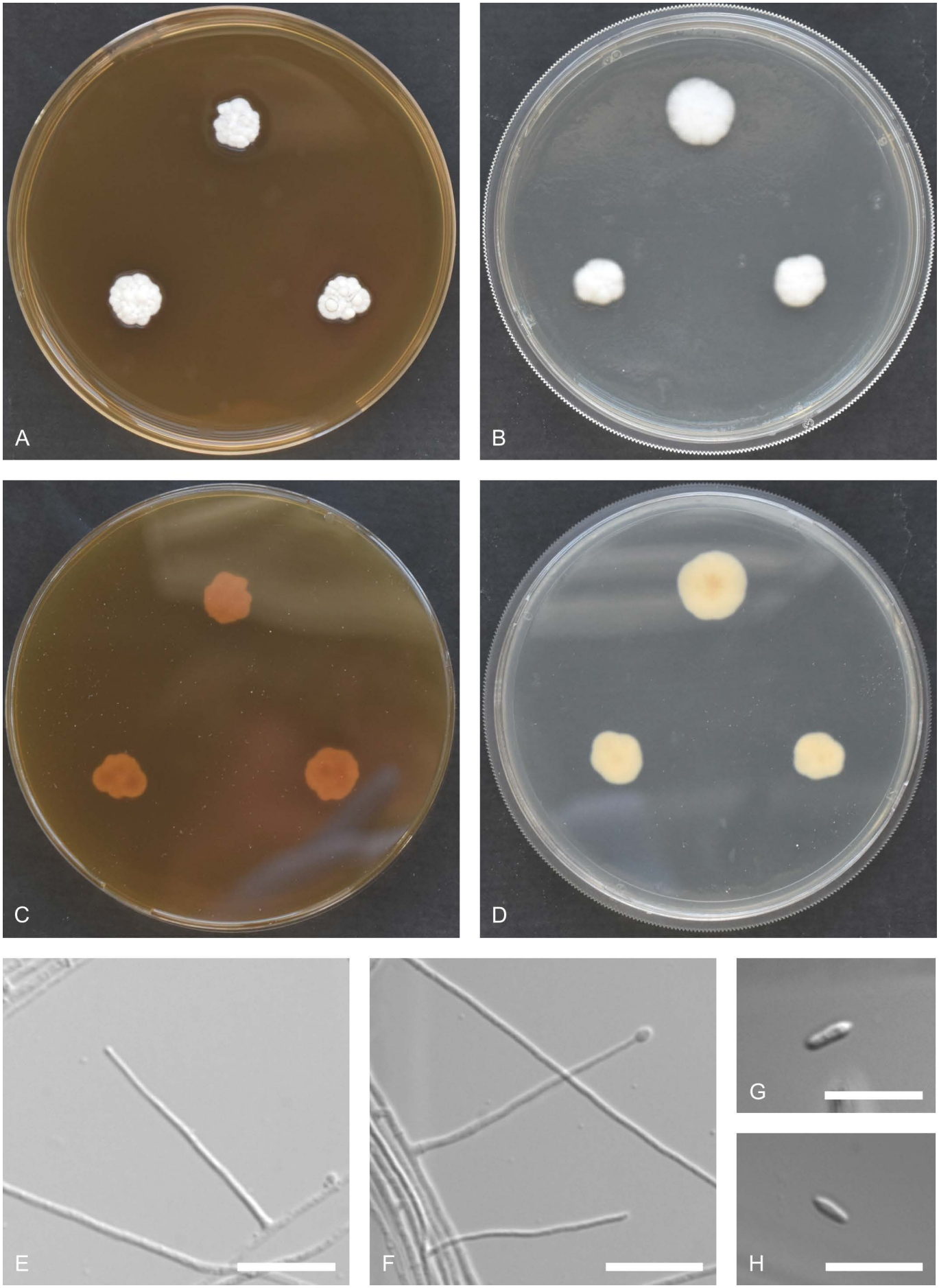

Fig. 15. Morphological features of *Lenticillium mouthense*. **A, B.** Upper views of the culture on MEA and PDA (10 d at 25 °C). **C, D.** Reverse views of the culture on MEA and PDA (10 d at 25 °C). **E–H.** Conidiogenous cells and conidia. Scale bars: E–H = 10 µm.

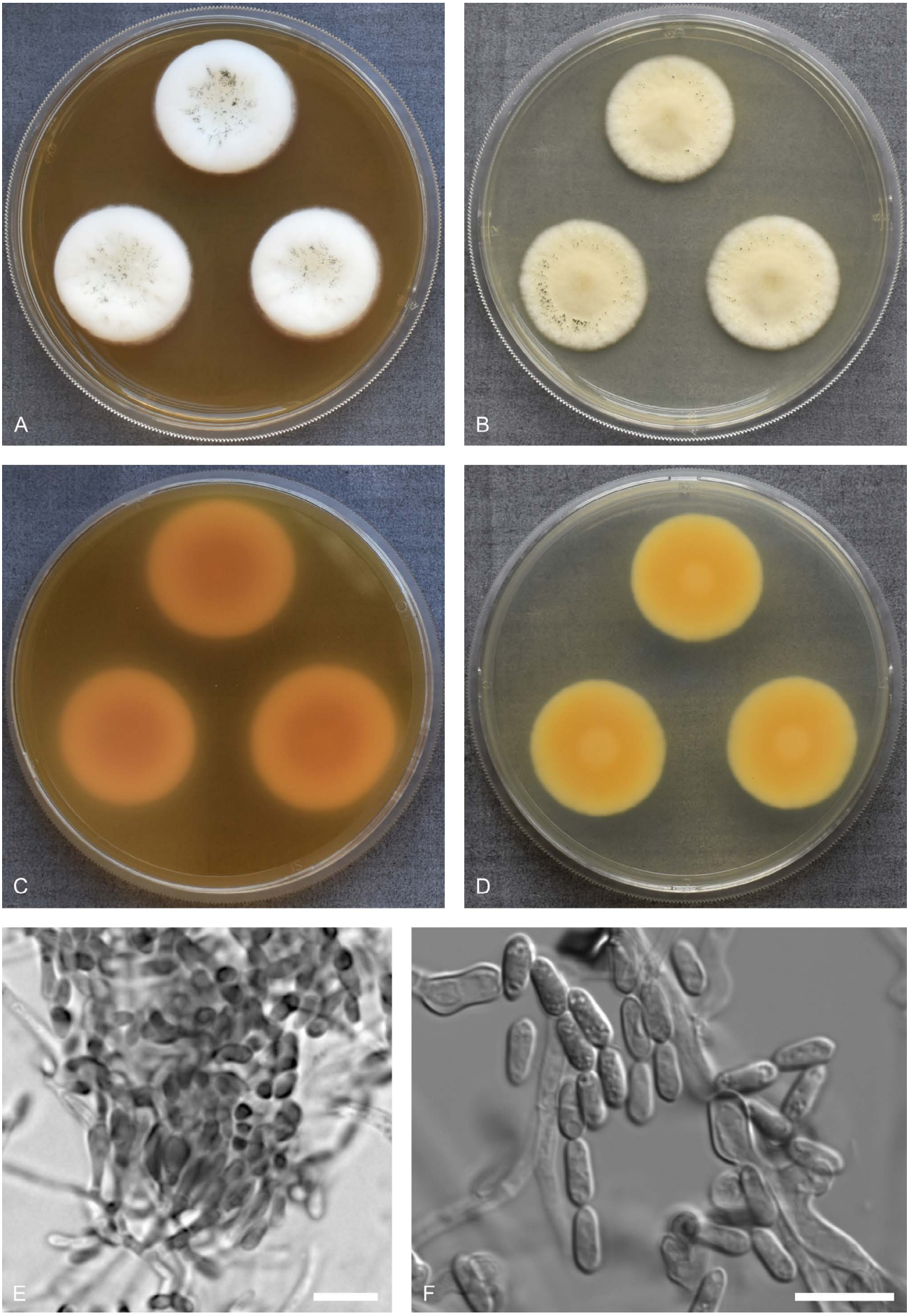

Fig. 16. Morphological features of *Metarhizium chabotense*. **A, B.** Upper views of the culture on MEA and PDA (10 d at 25 °C). **C, D.** Reverse views of the culture on MEA and PDA (10 d at 25 °C). **E.** Conidiogenous cells arranged in a candelabrum-like manner. **F.** Conidia. arranged in chains. Scale bars: E–F = 10 µm.

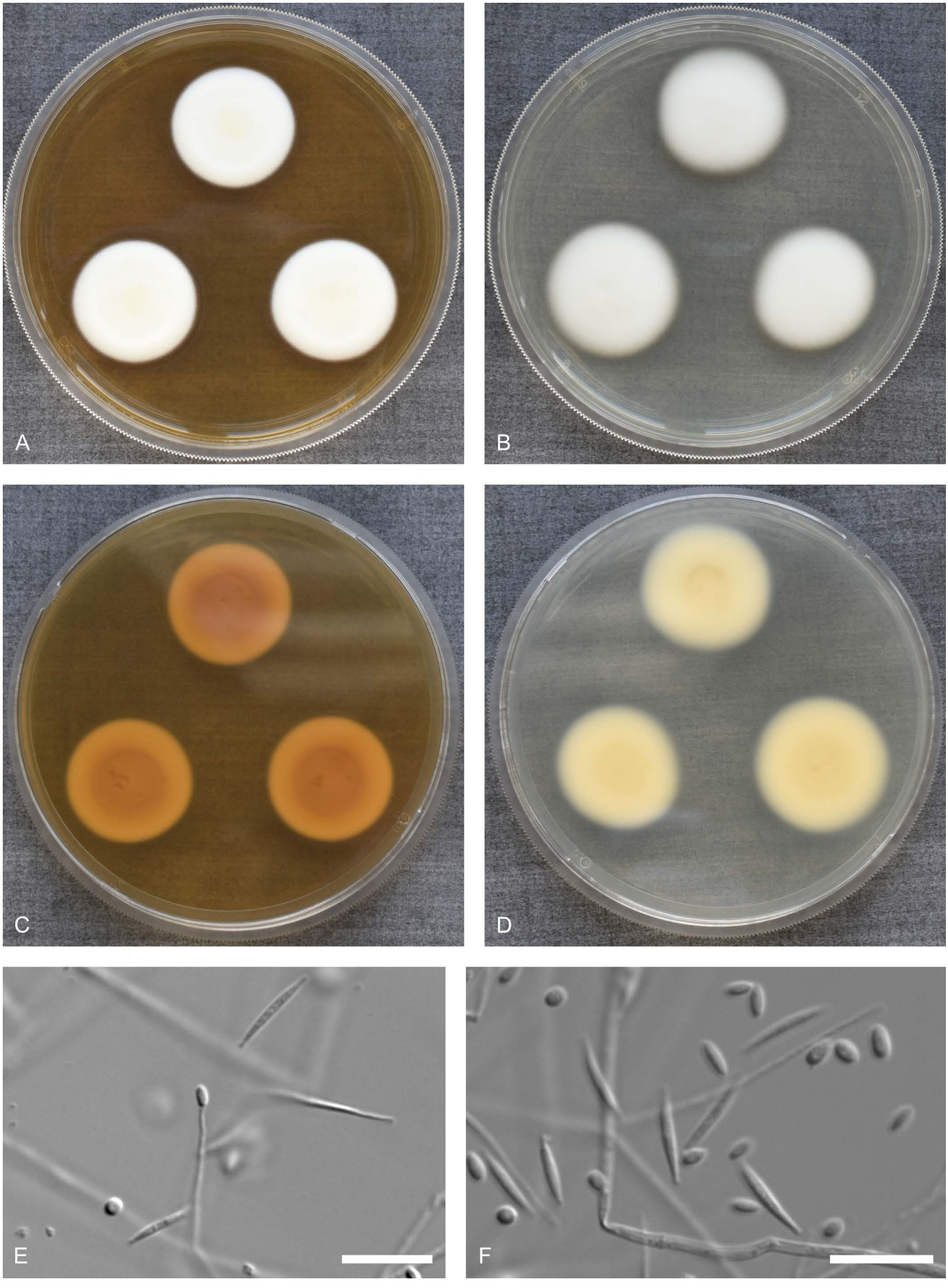

Fig. 17. Morphological features of *Simplicillium aquitainense*. **A, B.** Upper views of the culture on MEA and PDA (10 d at 25 °C). **C, D.** Reverse views of the culture on MEA and PDA (10 d at 25 °C). **E.** Conidiogenous cells arising laterally on prostrate hyphae. **F.** Fusiform macroconidia and microconidia of various shapes. Scale bars: E–F = 10 µm.

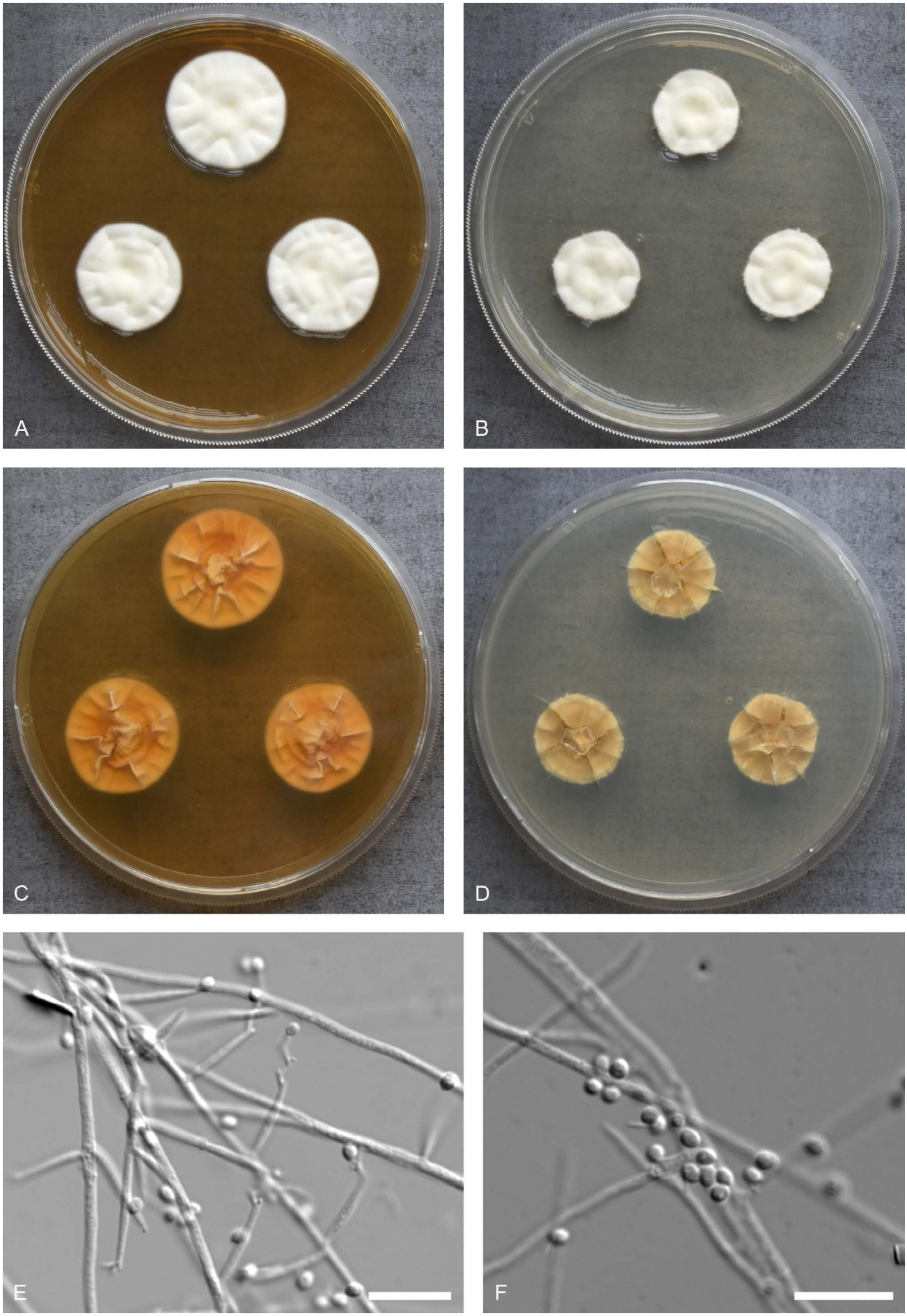

Fig. 18. Morphological features of *Simplicillium neosympodiophorum*. **A, B.** Upper views of the culture on MEA and PDA (10 d at 25 °C). **C, D.** Reverse views of the culture on MEA and PDA (10 d at 25 °C). **E, F.** Conidiogenous cells and conidia. The picture displays the typical zigzag-shaped portion of the conidiogenous cells. Scale bars: E–F = 10 µm.

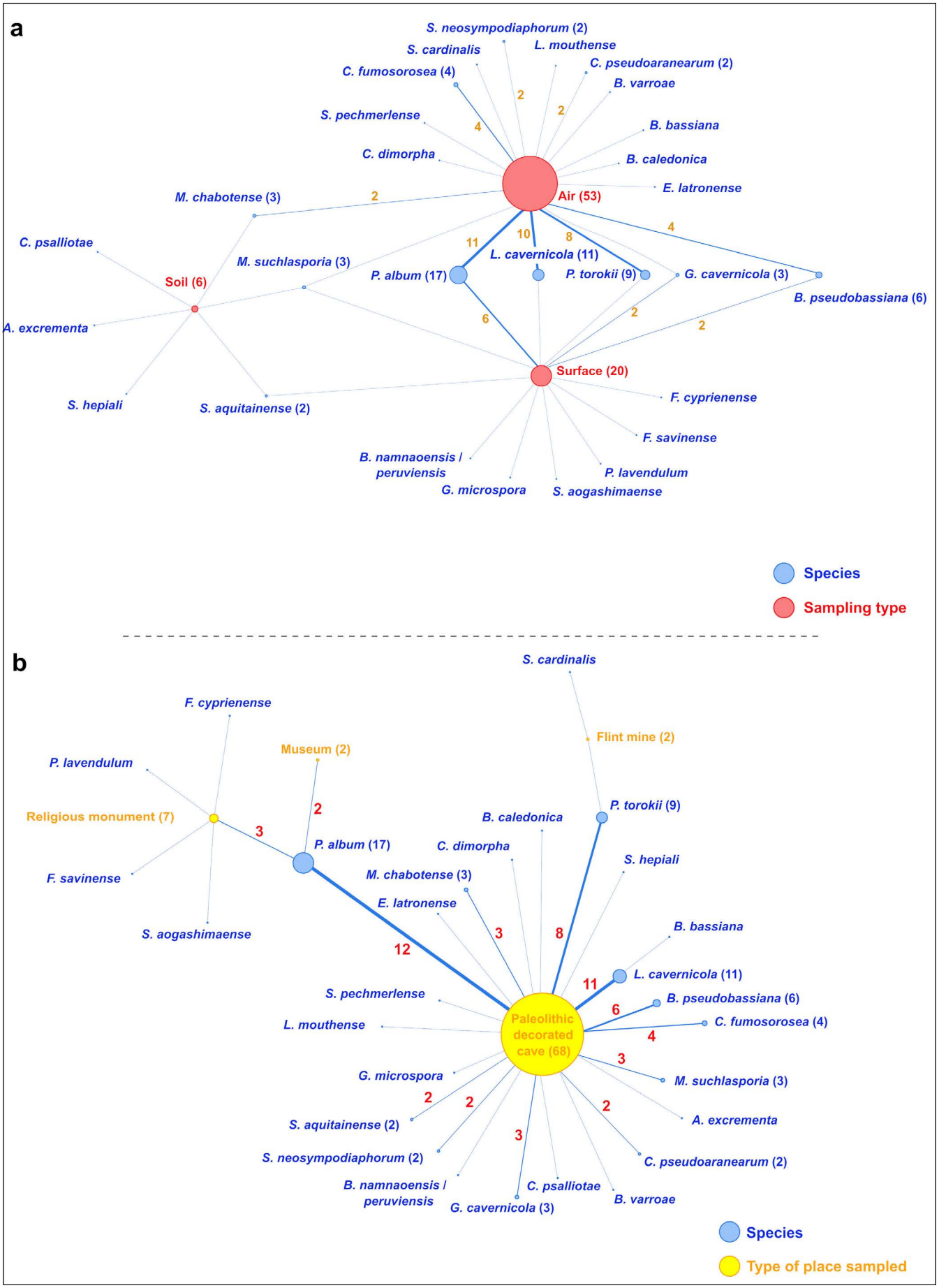

Fig. 19. Distribution of fungal species according to the sampling type and the type of place sampled. The figure depicts the distribution of fungal species according to the sampling type (a) and the type of place sampled (b). The size of the nodes as well as of the vertices is proportional to the number of relevant fungal strains. The numbers attributed to each node and to each vertex corresponds to the number of relevant fungal strains. This number is noted if it is greater than one.

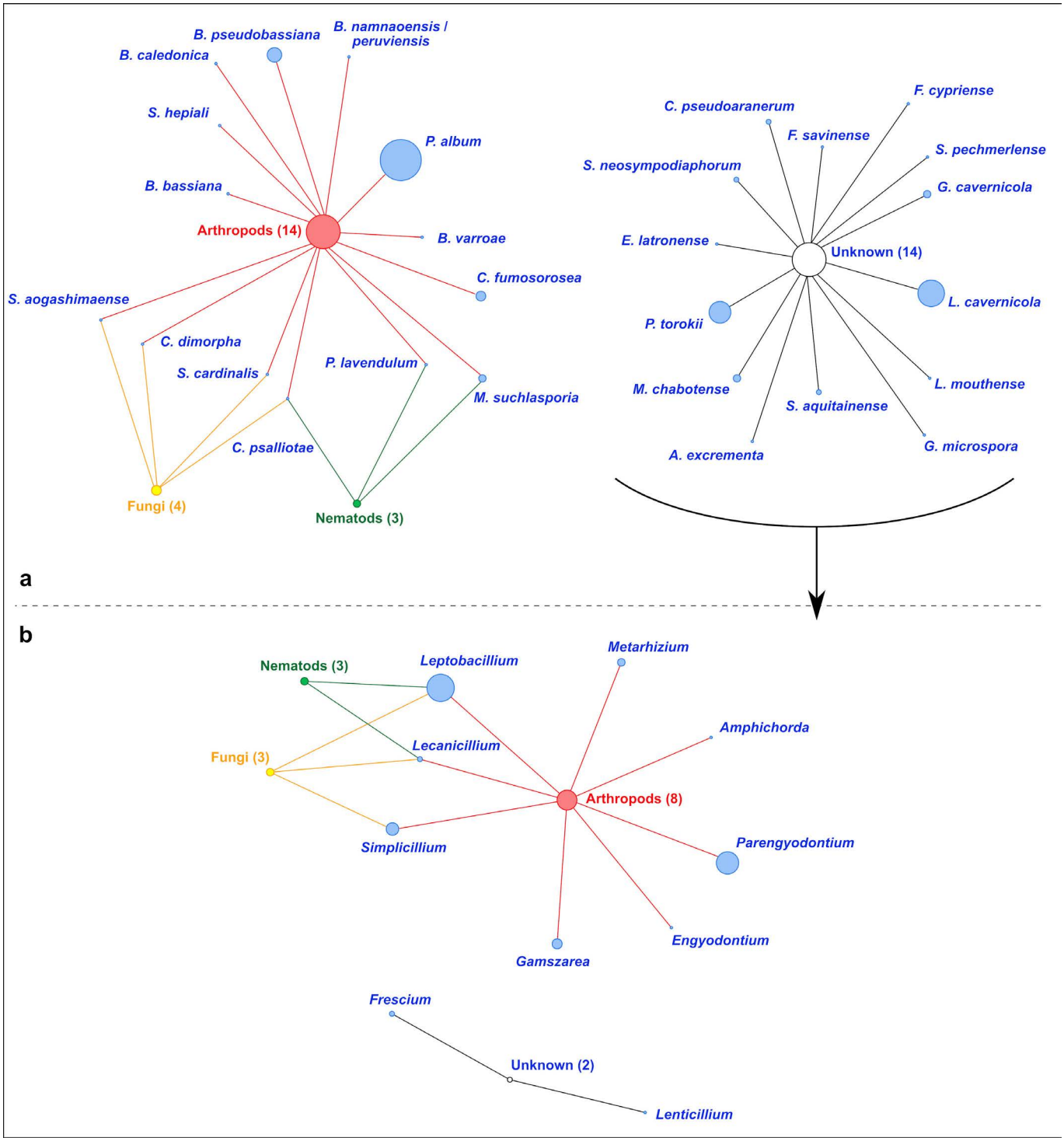

Fig. 20. Hosts related to isolated fungal strains. The figure depicts the known hosts of previously described fungal species (a), or the known hosts in the genera in the case of newly described species or for species with unknown host (b). The size of the nodes is proportional to the number of species (a) or genera (b) known for each type of host, or proportional to the number of strains isolated for each species (a) or each genus (b). The number of species or genera known as parasites is noted close to each host type.

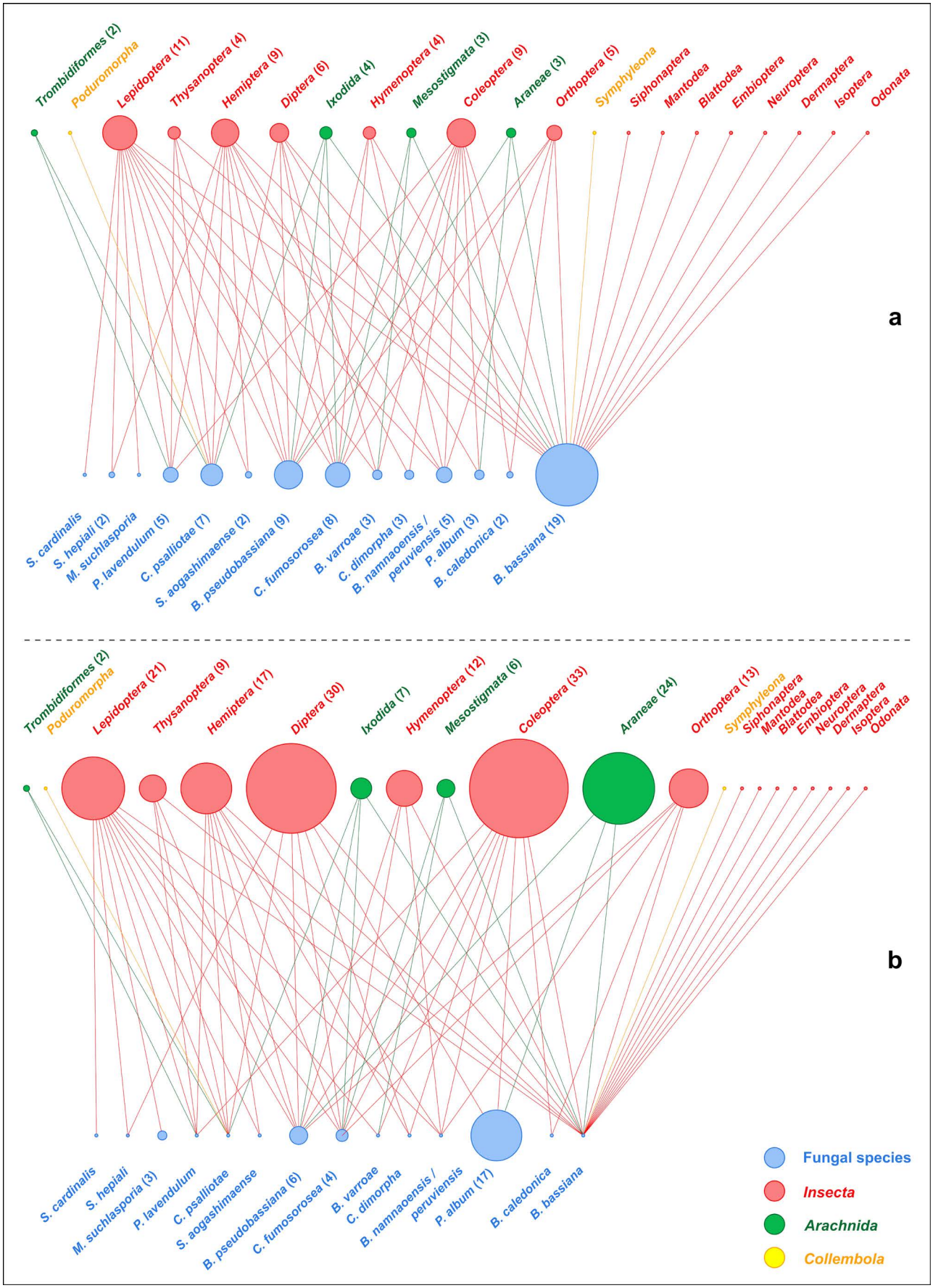

Figu. 21. Arthropod orders known as hosts for the isolated fungal strains. The figure depicts the orders among arthropods known to be hosts for each previously described fungal species isolated in this study. Different colours are used to differentiate between the *Insecta*, *Arachnida* and *Collembolla* arthropod orders. The size of the node for each species is proportional to the number of orders known to be hosts for this species (a) or to the number of strains identified in this species (b). Numbers greater than one are noted close to the species name and to the order name. The size of the node for each arthropod order is proportional to the number of fungal species known to be parasites for this order (a) or to the number of isolated strains known to be parasites for this order (b). This number is not noted close to the species name and to the order name when it is greater than one.

Description: *Colonies* on MEA reached 22–27 mm diam. at 25 °C, white to light yellow in the centre, velutinous to floccose, small amount of light yellow exudate sometimes present. Reverse brownish orange to light brown. Usually no growth at 30 °C. Colonies on PDA reached 23–29 mm diam. after 10 d at 25 °C, white, velutinous to floccose. Reverse white to light yellow. Usually no growth at 30 °C, but very small traces of growth are sometimes visible. *Hyphae* septate, smooth walled, hyaline. *Conidiogenous cells* arising laterally from prostrate hyphae, mostly solitary, occasionally in whorls of two, straight, tapering to the apex, 11.9–30.1 × 1.3–1.5 µm. *Conidia* aseptate, hyaline, smooth walled, variable in size and shape, microconidia subglobose, ellipsoidal, cylindrical or fusiform, 2.0–4.6 × 1.2–2.3 um, macroconidia fusiform, straight to slightly curved, 7.9–10.8 × 1.4–1.6 µm. *Octahedral crystals* absent.

Notes: *Simplicillium aquitainense* produces both microconidia and macroconidia as observed in *S. album*, *S. calcicola*, *S. lamellicola* and *S. pechmerlense*. Interestingly, *S. album*, *S. calcicola* and *S. pechmerlense* were all first isolated from the same environment as *S. aquitainense*, *i.e.* karst caves, suggesting the generally high occurrence of the genus *Simplicillium* in such environments, and maybe more specifically that of *Simplicillum* species producing both microconidia and macroconidia. *Simplicillium lamellicola* is distinguished from the other species by the production of octahedral crystals. *Simplicillium aquitainense* has a slower growth rate than *S. calcicola* and has larger macroconidia than *S. pechmerlense*. In comparison, the morphological distinction between *S. aquitainse* and *S. album* seems much more difficult despite the clear phylogenetic distinction, but the macroconidia produced by *S. aquitainense* do seem thinner than those produced by *S. album* (Zhang *et al.* 2020). *Simplicillium album* and *S. aquitainense* formed two sister clades, which both were supported in 100 % of the bootstraps and with a posterior probability of 1.00 (Fig. 6). These two different clades are the result of 66 different bp when considering the concatenation of ITS, nrLSU and *tef-1α* sequences, no sequence being available for *S. album rpb1* and *rpb2* regions.

Other strains examined: **France**, LRMH C159, Sainte-Anastasie, 43°55’49”N, 4°20’04”E, Sep. 2015, isolated from soil sampling in Baume Latrone Cave, collected and isolated by the microbiologists of the French Historical Monuments Research Laboratory.

Simplicillium neosympodiophorum J. Leplat, ***sp. nov.*** MB 850851. Fig. 18.

Etymology: The epithet *neosympodiophorum* refers to the sympodial production of microconidia by conidiogenous cells in this species. This species is only the second in *Simplicillium* after *S. sympodiophorum* to express such sympodial growth.

GenBank: OR264327 (ITS), OR263661 (nrLSU), OR269659 (*rpb1*), OR291092 (*rpb2*), OR291130 (*tef-1α*).

Typus: **France**, Sainte-Anastasie, 43°55’49”N, 4°20’04”E, Jul. 2021, isolated from air sampling in Baume Latrone cave, collected and isolated by the microbiologists of the French Historical Monuments Research Laboratory (**holotype** CBS 150568, preserved in a metabolically inactive state), culture ex-type CBS 150568 = LRMH C465.

Known distribution: France, Occitanie region.

Description: *Colonies* on MEA reached 22–26 mm diam. at 25 °C, white, velutinous to floccose, radially striate. Reverse light orange to deep orange. Colonies reached 5–8 mm diam. at 30 °C. Colonies on PDA reached 18–20 mm diam. at 25 °C, white, velutinous to floccose, radially striate. Reverse white to light brown. Colonies reached 10–13 mm diam. 30 °C. *Hyphae* septate, smooth walled, hyaline. *Conidiogenous cells* arising laterally from prostrate hyphae, mostly solitary, tapering to the apex, terminating in a fertile zigzag-shaped portion bearing microconidia on denticles, 17.1–20.9 × 1.0–1.5 um. *Conidia* aseptate, hyaline, smooth-walled, subglobose to ellipsoidal, 2.0–2.9 × 1.5–1.7 um. *Octahedral crystals* absent.

Notes: *Simplicillium neosympodiophorum* is the second species after *S. sympodiophorum* to express a sympodial growth of microconidia in the genus *Simplicillium*. *Simplicillium neosympodiophorum* is easily distinguishable from *S. sympodiophorum* by the shape of the fertile region of conidiogenous cells: while this region is straight in *S. sympodiophorum*, it is a clear zigzag shape in *S. neosympodiophorum*, and resembles the shape encountered in *Parengyodontium* species (Nonaka *et al*. 2013, Leplat *et al.* 2022a). Conidiogenous cells produced by *S. neosympodiophorum* also seem shorter than those produced by *S. sympodiophorum*. *Simplicillium aogashimaense* is the closest species from *S. neosympodiophorum* phylogenetically (Fig. 6). These two species formed two sister clades, which both were supported in 100 % of the bootstraps and with a posterior probability of 1.00. These two different clades are the result of 70 different bp when considering the concatenation of ITS, nrLSU and *tef-1α* sequences, no sequence being available for *S. aogashimaense rpb1* and *rpb2* regions.

Other strains examined: **France**, LRMH C195, Sainte-Anastasie, 43°55’49”N, 4°20’04”E, June 2016, isolated from air sampling in Baume Latrone Cave, collected and isolated by the microbiologists of the French Historical Monuments Research Laboratory.

DISCUSSION

Overview of the distribution of the isolated species

Among the 79 fungal strains studied, 53 were recovered through air samplings, 20 through surface sampling and six through soil samplings (Fig. 19a). Many species were only isolated once, through a single sampling method. *Metapochonia suchlasporia* var. *suchlasporia* was the only species that was isolated through all three sampling methods, as found in previous studies (Vaughan *et al*. 2011, Martin-Sanchez *et al.* 2014, Mitova *et al.* 2017). The species that were the most frequently isolated were in general recovered from both air and surface sampling, such as *Parengyodontium album* or *Leptobacillium cavernicola*, showing that the oc-

currence of these species can be detected through several sampling methods.

In general, all strains belonging to the same fungal species were isolated from the same type of environment (Fig. 19b). The only exception was *Parengyodontium album*, which was isolated from Paleolithic decorated caves, from religious monuments and from a museum. This fungal species is known to be ubiquitous in a cultural heritage context, and in particular on monuments suffering from salt crystallization problems (Leplat *et al.* 2020a). To our knowledge, this is the first time to date that the presence of *Amphichorda excrementa*, *Beauveria caledonica*, *B. namnoensis/ peruviensis*, *Corniculantispora dimorpha*, *Samsoniella cardinalis* and *S. hepiali* has been reported among the species isolated from the cave environment (Paleolithic decorated caves and a flint mine), while the presence of *Beauveria bassiana*, *B. pseudobassiana*, *B. varroae*, *Cordyeps fumosorosea*, *Corniculantispora psalliotae*, *Gamszarea microspora*, *Metapochonia suchlasporia* and *Parengyodontium album* had already been noted in this environment (Bastian *et al.* 2009, Nováková 2009, Zhang *et al.* 2020, Sanchez-Moral *et al.* 2021). Moreover, the presence of *A. excrementa*, *B. caledonica*, *B. namnoensis/peruviensis*, *S. cardinalis* and *S. hepialid* had never been reported in a cultural heritage context in general, while *C. dimorpha* had already been detected in the air of historical archive environments (Pavlović *et al.* 2023). Although the presence of *Leptobacillum cavernicola* and *Parengyodontium torokii* in caves had not yet been reported with these species names by other authors (the species in question were recently segregated from *L. leptobactrum* and *P. album* (Leplat *et al.* 2022b, Parker *et al.* 2022), they had certainly already been detected there and had been sorted under their former names (Leplat *et al.* 2022a, b). *Purpureocilllium lavendulum* and *Simplicillium aogashimaense* were isolated from surface samples in religious monuments. This is consistent with a previous study regarding *P. lavendulum*, which was isolated from the walls of the cathedral of Coimbra (Trovão *et al.* 2019), while the only mention of *S. aogashimaense* in relation with cultural heritage was its strong presence on a piece of pottery excavated from the soil (Ren *et al.* 2023).

Among the newly described species, *Corniculantispora pseudoaraneaeum, Engyodontium latronense*, *Gamszarea cavernicola*, *Lenticillium mouthense*, *Metarhizium chabotense*, *Simplicillium aquitainense* and *Simplicillium neosypodiaphorum* were all isolated from caves. With the exception of the newly described genus *Lenticillium*, all of these genera had already been recovered in caves (Kubátová & Dvorák 2005, Zhang *et al.* 2017, 2020, Novakova *et al*. 2018, Stupar *et al.* 2023). Finally, regarding the newly described genus *Frescium*, the two species of this genus were recovered in the same place, *i.e.* a church crypt, which supports the hypothesis that the two species have close ecological requirements.

Link between fungal species and their possible hosts

One of the aims of the study was to evaluate if the presence of the isolated species could provide data about the presence of their hosts in the cultural heritage monuments considered. The species isolated in this study are reputed to be parasites of arthropods, fungi and nematodes (Fig. 20a). Only one of the known species, *Corniculantispora psalliotae*, is known to be a parasite of all three types of host (Zare & Gams 2001, Yang *et al.* 2005, Sukarno *et al.* 2009).

Metapochonia suchlasporia and *Purpurocillium lavendulum* are known to be mainly parasites of nematodes, but sometimes also of arthropods (Evans & Kirk 2017, Bao *et al.* 2022). The presence of these two genera could therefore be linked to the presence of nematodes in cultural heritage sites, and notably in caves in the case of *M. suchlasporia*. Indeed, the presence of nematodes has already been reported in caves, although there are few studies on the subject to date (Du Preez *et al.* 2017).

Corniculantispora dimorpha and *Simplicillium aogashimaense* are mainly known to be fungicolous (Zare & Gams 2001, Zhu *et al.* 2022), but they can certainly also be parasites of some arthropods (Gielen *et al.* 2021, Mantzoukas *et al.* 2023). *Corniculantispora dimorpha* was isolated from *Agaricus bisporus*, the cultivated mushroom, and from *Puccinia coronata*, the causal agent of oat crown rust (Zare & Gams 2001). The former is a macrofungus and the latter a microfungus; both of these species have affiliations to the *Basidiomycota*. As is the case for *C. dimorpha,* these genera have already been detected in caves, and sometimes in large amounts (Docampo *et al.* 2011). The presence of *C. dimorpha* in caves may therefore be due to the presence of other fungi in these caves. Conversely, *Samsoniella cardinalis* was first isolated from arthropods (Wang *et al.* 2020b), but has since also been isolated from fungi (Chuang *et al.* 2024).

The eight remaining identified species are only known to be parasites of arthropods (de Faria & Wraight 2007, Rehner *et al.* 2011, Trovão *et al.* 2013, Yoder *et al*. 2017, Bustamante *et al.* 2019, Weng *et al*. 2019, Wang *et al.* 2020a, b, Kobmoo *et al.* 2021).

Among the newly described species or species with unknown host, the host range of the corresponding genera was very similar to that of previously known species (Fig. 20b). Two genera are known to be parasites of arthropods, fungi and nematodes: *Corniculantispora* (as already observed for *C. psalliotae*) and *Leptobacillium* (Zare & Gams 2016, Okane *et al.* 2020). The genus *Simplicillium* has previously been described as a parasite of fungi and arthropods. And in addition to the genus *Parengyodontium*, the genera *Amphichorda*, *Engyodontium*, *Gamszarea* and *Metarhizium* are also well-known parasites of arthropods (Gams *et al.* 1984, Roberts & Leger 2004, Zhang *et al.* 2020, Ramanujam *et al.* 2021). Finally, *Frescium* and *Lenticillium* are newly described, and as such, are the only genera with an unknown host range.

As all isolated strains are likely to be entomogenous strains, a more detailed analysis had to be performed regarding arthropods (Fig. 21). A large host range has been observed in some of the fungal species identified (Fig. 21a), such as *Beauveria bassiana*, which is known to parasite at least 19 arthropod orders (Zimmermann 2007). Conversely, some species were recovered from only one arthropod order, including *Samsoniella hepiali* and *Metapochonia suchlasporia*, which were recovered from *Lepidoptera* (Humber *et al.* 2005, Wang *et al*. 2020b). The order *Lepidoptera* was found to be a host for the majority of the fungal species identified, since 11 out of the 14 identified species were recovered on this order. Besides *Lepidopera*, *Coleoptera* (9), *Hemiptera* (9) and *Diptera* (6)

were recognized as hosts for the majority of the fungal species identified. Conversely, 10 of the 21 arthropod orders identified as hosts for the isolated species are parasitized by only one of these species, often *B. bassiana*.

When the number of strains isolated in each fungal species was taken into account (Fig. 21b), *Coleoptera* corresponded to the highest number of strains isolated (33), followed by *Diptera* (30) and *Araneae* (24), with *Lepidoptera* coming fourth with 21 strains that were known to be parasites. These results are due to the 17 isolated strains of *Parengyodontium album*, the most frequently isolated species, since this species has only been recovered on *Coleoptera*, *Diptera* and *Araneae* (Trovão *et al.* 2013, Jaber *et al.* 2016, Teixeira *et al.* 2020). Thus, *Araneae* was the possible host of 24 strains, which corresponded to only three species, while *Lepidoptera* was the possible host of 21 strains that corresponded to 11 species.

These results reflect to some extent what is currently known about the diversity of arthropods in caves, where most of the species isolated in this study were found. *Diptera*, *Coleoptera* and *Araneae*, which were the possible hosts for the greatest number of isolated strains, are indeed the most abundantly recovered arthropod orders in cave surveys (Mammola *et al.* 2017, Wynne *et al*. 2018, Balestra *et al.* 2021, Evans *et al.* 2024). *Acari* and *Collembolla* are the possible hosts of only 15 and two strains respectively and are under-represented hosts despite their relative abundance in cave environments. Indeed, *Acari* and *Collembolla* are considered to be the most abundant arthropods in caves (Gers 1998). The same is true to a lesser extent for *Orthoptera*, which is usually among the most abundant orders in caves (Howarth 2009), but which was found to be the possible host of only 13 strains representing five different fungal species, four of which belong to *Beauveria*. In contrast, the order *Lepidoptera* seems a little over-represented insofar that it was the possible host of 21 strains belonging to 11 species. While this order is frequent in caves, it is not among the most abundant orders (Wynne *et al*. 2018, Balestra *et al.* 2021). This result could be linked to the increased use of caves by butterflies and moths over the past few years (Moog *et al.* 2021). Finally, among the arthropod orders defined as known hosts of identified fungal species, *Mantodea* is the only order that had never been isolated from a cave environment. However, the occurrence and abundance of *Thysanoptera*, *Embioptera*, *Neuroptera*, *Dermaptera*, *Isoptera*, *Odonata* and *Siphonaptera* in caves was weak (de Oliveira Motta *et al*. 2001, Bento *et al.* 2016, Wynne *et al.* 2018, Balestra *et al.* 2021). This result was expected since all of these orders, with the exception of *Thysanoptera,* were the possible hosts of *Beauveria bassiana* alone, which was only isolated once. As for *Thysanoptera*, it was the possible host of nine strains including *Beauveria pseudobassiana*, which was isolated six times from different caves. It is therefore probable that the host of these strains was not *Thysanoptera*, but another order among the seven known to host this fungal species.

In the case of caves, the isolated fungal species do therefore seem to be reliable indicators of the arthropods present, but this hypothesis remains to be confirmed by simultaneous studies on fungi and arthropods. Studies considering both the identification of fungi and of their hosts are scarce and incomplete for cave environments, and even more so in the cultural heritage environment. Few studies simultaneously identified the hosts and the fungal species recovered on them (Kubátová & Dvorák 2005), and most of these studies focused on one particular host (Gunde-Cimerman *et al*. 1998, Santamaria & Faille 2007, Evans *et al.* 2024). In others, the host was precisely identified but the fungal species were identified only at the genus level, such as *Beauveria* spp. recovered on the cave cricket and the cave spider (Benoit *et al.* 2004, Yoder *et al.* 2009). Studies often noted that fungal species were recovered from arthropods, but did not identify the latter (Nováková 2009, Vanderwolf *et al*. 2013). Most of the studies recovered fungal species that were known to be entomopathogenic and thus made hypotheses about the role of arthropods (Jurado *et al.* 2008, Bastian *et al*. 2009, Dominguez-Moñino *et al*. 2021), as we do in this study. The attempts to link fungal species to hosts are even scarcer when studies concern sites other than caves (Gorbushina & Petersen 2000, Trovão *et al.* 2013). These studies mainly seek to highlight the role of arthropods in the dissemination of fungi on monuments. This question is a major concern when dealing with the fungal biodeterioration of monuments, especially since the relation between the concentration of airborne fungal spores and arthropod populations had already been proven for other fungal species/arthropod species combinations (Magyar *et al*. 2023). However, the question of a direct link between fungal dissemination by arthropods and the development of biodeterioration phenomena on cultural heritage monuments has still to be studied.

ACKNOWLEDGEMENTS

Financial support for the OPerCul workstation used to perform the robustness calculations for the phylogenetic studied was provided by the Paris Ile-de-France Region – DIM “Matériaux anciens et patrimoniaux”. The microscopic pictures were taken in the Centre de Microscopie et Imagerie du Muséum (CeMIM), UMR 7245 Muséum National d’Histoire Naturelle, 57 rue Cuvier, 75005 Paris, France. We thank Joanna Lignot from Munro Language Services for English language editing.

Declaration on conflict of interest The authors have no conflict of interest to disclose.

REFERENCES

Alonso L, Pommier T, Simon L, *et al.* (2022). Microbiome analysis in Lascaux cave in relation to black stain alterations of rock surfaces and collembola. *Environmental Microbiology Reports* **15**: 80–91. https://doi.org/10.1111/1758-2229.13133

Araújo JPM, Lebert BM, Vermeulen S, *et al.* (2022). Masters of the manipulator: two new hypocrealean genera, *Niveomyces* (*Cordycipitaceae*) and *Torrubiellomyces* (*Ophiocordycipitaceae*), parasitic on the zombie ant fungus *Ophiocordyceps camponoti-floridani*. *Persoonia* **49**: 171–194. https://doi.org/10.3767/persoonia.2022.49.05

Balestra V, Lana E, Carbone C, *et al.* (2021). Don’t forget the vertical dimension: assessment of distributional dynamics of cave-dwelling invertebrates in both ground and parietal microhabitats. *Subterranean Biology* **40**: 43–63. https://doi.org/10.3897/subtbiol.40.71805

Bao ZX, Liu R, Li CQ, *et al.* (2022). Pathogenicity and metabolites of *Purpureocillium lavendulum* YMF1. 00683 against *Meloidogyne incognita*. *Pathogens* **11**: 795. https://doi.org/10.3390/pathogens11070795

Bastian F, Alabouvette C (2009). Lights and shadows on the conservation of a rock art cave: the case of Lascaux Cave. *International Journal of Speleology* **38**: 55–60. https://doi.org/10.5038/1827-806X.38.1.6

Bastian F, Alabouvette C, Saiz-Jimenez C (2009). The impact of arthropods on fungal community structure in Lascaux Cave. *Journal of Applied Microbiology* **106**: 1456–1462. https://doi.org/10.1111/j.1365-2672.2008.04121.x

Bastian F, Jurado V, Nováková A, *et al.* (2010). The microbiology of Lascaux cave. *Microbiology* **156**: 644–652. https://doi.org/10.1099/mic.0.036160-0

Benoit JB, Yoder JA, Zettler LW, *et al.* (2004). Mycoflora of a trogloxenic cave cricket, *Hadenoecus cumberlandicus* (*Orthoptera*: *Rhaphidophoridae*), from two small caves in northeastern Kentucky. *Annals of the Entomological Society of America* **97**: 989–993. https://doi.org/10.1603/0013-8746(2004)097%5B0989:MOATCC%5D2.0.CO;2

Bensch K, Braun U, Groenewald JZ, *et al.* (2012). The genus *Cladosporium*. *Studies in Mycology* **72**: 1–401. https://doi.org/10.3114/sim0003

Bento DM, Ferreira RL, Prous X, *et al.* (2016). Seasonal variations in cave invertebrate communities in the semiarid Caatinga, Brazil. *Journal of Cave and Karst Studies* **78**: 61–71. https://doi.org/10.4311/2015LSC0111

Bischoff JF, Rehner SA, Humber RA (2009). A multilocus phylogeny of the *Metarhizium anisopliae* lineage. *Mycologia* **101**: 512–530. https://doi.org/10.3852/07-202

Bustamante DE, Oliva M, Leiva S, *et al.* (2019). Phylogeny and species delimitations in the entomopathogenic genus *Beauveria (Hypocreales*, *Ascomycota*), including the description of *B. peruviensis sp. nov*. *MycoKeys* **58**: 47–68. https://doi.org/10.3897/mycokeys.58.35764

Chuang W, Lin Y, Shrestha B, *et al.* (2024). Phylogenetic diversity and morphological characterization of cordycipitaceous species in Taiwan. *Studies in Mycology* **109**: 1–56. https://doi.org/10.3114/sim.2024.109.01

Clark K, Karsch-Mizrachi I, Lipman DJ, *et al.* (2016). GenBank. *Nucleic Acids Research* **44**: D67–D72. https://doi.org/10.1093/nar/gkv1276

Colmán A, Araújo J, Evans H, *et al.* (2025). Hidden diversity behind the lecanicillium-like white colony-forming mycoparasites on *Hemileia vastatrix* (coffee leaf rust). *Persoonia* **55**: 239–275. https://doi.org/10.3114/persoonia.2025.55.07

Crous PW, Verkley GJM, Groenewald JZ, *et al.* (2009). *Fungal Biodiversity*. CBS Laboratory Manual Series No 1. Westerdijk Fungal Biodiversity Institute, Utrecht, The Netherlands.

Culver DC, Pipan T (2018). Insects in caves. In: *Insect Biodiversity: Science and Society* (Foottit, RG, Adler, PH eds.). John Wiley & Sons, Hoboken (USA): 123–152.

de Faria MR, Wraight SP (2007). Mycoinsecticides and mycoacaricides: a comprehensive list with worldwide coverage and international classification of formulation types. *Biological Control* **43**: 237–256. https://doi.org/10.1016/j.biocontrol.2007.08.001

de Hoog GS (1978). Notes on some fungicolous Hyphomycetes and their relatives. *Persoonia* **10**: 33–81.

De Leo F, Marchetta A, Urzì C (2022). Black fungi on stone-built heritage: current knowledge and future outlook. *Applied Sciences* **12**: 3969. https://doi.org/10.3390/app12083969

de Oliveira Motta JA, Ferreira RL, Silva MS, *et al.* (2001). Biological survey of cave invertebrates in the project: *"Cavernas de Mambaí"-Mambaí, Posse, Buritinópolis and Damianópolis, Goiás State, Brazil*.

Docampo S, Trigo M, Recio M, *et al.* (2011). Fungal spore content of the atmosphere of the Cave of Nerja (southern Spain): diversity and origin. *Science of the Total Environment* **409**: 835–843. https://doi.org/10.1016/j.scitotenv.2010.10.048

Dominguez-Moñino I, Jurado V, Rogerio-Candelera MA, *et al.* (2021). Airborne fungi in show caves from southern Spain. *Applied Sciences* **11**: 5027. https://doi.org/10.3390/app11115027

Du Preez G, Majdi N, Swart A, *et al.* (2017). Nematodes in caves: a historical perspective on their occurrence, distribution and ecological relevance. *Nematology* **19**: 627–644. https://doi.org/10.1163/15685411-00003068

Edel V, Steinberg C, Gautheron N, *et al.* (2001). Genetic diversity of *Fusarium oxysporum* populations isolated from different soils in France. *FEMS Microbiology Ecology* **36**: 61–71. https://doi.org/10.1016/S0168-6496(01)00119-2

Edler D, Klein J, Antonelli A, *et al.* (2021). raxmlGUI 2.0: a graphical interface and toolkit for phylogenetic analyses using RAxML. *Methods in Ecology and Evolution* **12**: 373–377. https://doi.org/10.1111/2041-210X.13512

Evans H, Fogg T, Buddie A, *et al.* (2024). The araneopathogenic genus *Gibellula* (*Cordycipitaceae: Hypocreales*) in the British Isles, including a new zombie species on orb-weaving cave spiders (*Metainae: Tetragnathidae*). *Fungal Systematics and Evolution* **15**: 153–178. https://doi.or/10.3114/fuse.2025.15.07

Evans HC, Kirk PM (2017). Systematics of *Pochonia*. In: *Perspectives in Sustainable Nematode Management through Pochonia Chlamydosporia Applications for Root and Rhizosphere Health* (Manzanilla-López, RH, Lopez-Llorca, LV eds.). Springer (USA), New York: 21–43.

Gams W, De Hoog GS, Samson RA, *et al.* (1984). The hyphomycete genus *Engyodontium* a link between *Verticillium* and *Aphanocladium*. *Persoonia* **12**: 135–147.

Gers C 1998. Diversity of energy fluxes and interactions between arthropod communities: from soil to cave. *Acta Oecologica* **19**: 205–213. https://doi.org/10.1016/S1146-609X(98)80025-8

Gielen R, Meister H, Tammaru T, *et al.* (2021). Fungi recorded on folivorous *Lepidoptera*: high diversity despite moderate prevalence. *Journal of Fungi* **7**: 25. https://doi.org/10.3390/jof7010025

Gorbushina AA, Petersen K (2000). Distribution of microorganisms on ancient wall paintings as related to associated faunal elements. *International Biodeterioration & Biodegradation* **46**: 277–284. https://doi.org/10.1016/S0964-8305(00)00103-7

Green PWC (2008). Fungal isolates involved in biodeterioration of book-paper and their effects on substrate selection by *Liposcelis bostrychophila* (Badonnel) (*Psocoptera*:

Liposcelididae). *Journal of Stored Products Research* **44**: 258–263. https://doi.org/10.1016/j.jspr.2008.01.003

Gunde-Cimerman N, Zalar P, Jeram S (1998). Mycoflora of cave cricket *Troglophilus neglectus* cadavers. *Mycopathologia* **141**: 111–114. https://doi.org/10.1023/A:1006947524503

Hall TA (1999). BioEdit: a user-friendly biological sequence alignment editor and analysis program for Windows 95/98/NT. *Nucleic Acids Symposium Series* **41**: 95–98.

Howarth FG (2009). Cave insects. In: *Encyclopedia of Insects* (Resh, VH, Cardé, RT eds.). Elsevier (The Netherlands), Amsterdam: 139–143.

Humber RA, Hansen KS, Wheeler MM (2005). ARSEF index: Host-by-fungus. 2005. (http://www.arsef.fpsnl.cornell.edu/mycology/ARSEF).

Jaber S, Mercier A, Knio K, *et al.* (2016). Isolation of fungi from dead arthropods and identification of a new mosquito natural pathogen. *Parasites & Vectors* **9**: 491. https://doi.org/10.1186/s13071-016-1763-3

Jurado V, Fernandez-Cortes A, Cuezva S, *et al.* (2009). The fungal colonisation of rock-art caves: experimental evidence. *Naturwissenschaften* **96**: 1027–1034. https://dio.org/10.1007/s00114-009-0561-6

Jurado V, Sanchez-Moral S, Saiz-Jimenez C (2008). Entomogenous fungi and the conservation of the cultural heritage: a review. *International Biodeterioration & Biodegradation* **62**: 325–330. https://doi.org/10.1016/j.ibiod.2008.05.002

Katoh K, Rozewicki J, Yamada KD (2019). MAFFT online service: multiple sequence alignment, interactive sequence choice and visualization. *Briefings in Bioinformatics* **20**: 1160–1166. https://doi.org/10.1093/bib/bbx108

Kepler RM, Luangsa-Ard JJ, Hywel-Jones NL, *et al.* (2017). A phylogenetically-based nomenclature for *Cordycipitaceae* (*Hypocreales*). *IMA Fungus* **8**: 335–353. https://doi.org/10.5598/imafungus.2017.08.02.08

Khonsanit A, Thanakitpipattana D, Mongkolsamrit S, *et al.* (2024). A phylogenetic assessment of *Akanthomyces sensu lato* in *Cordycipitaceae* (*Hypocreales*, *Sordariomycetes*): introduction of new genera, and the resurrection of *Lecanicillium*. *Fungal Systematics and Evolution* **14**: 271–305. https://doi.org/10.3114/fuse.2024.14.17

Kobmoo N, Arnamnart N, Pootakham W, *et al.* (2021). The integrative taxonomy of *Beauveria asiatica* and *B. bassiana* species complexes with whole-genome sequencing, morphometric and chemical analyses. *Persoonia* **47**: 136–150. https://doi.org/10.3767/persoonia.2021.47.04

Kornerup A, Wanscher JH (1967). Methuen handbook of colour. (2nd ed.), *Methuen* & Co., London.

Kubátová A, Dvorák L (2005). Entomopathogenic fungi associated with insect hibernating in underground shelters. *Czech Mycology* **57**: 221–237. https://doi.org/10.33585/cmy.57303

Kumar S, Stecher G, Suleski M, *et al.* (2024). MEGA12: Molecular Evolutionary Genetic Analysis version 12 for adaptive and green computing. *Molecular Biology and Evolution* **41**: msae263. https://doi.org/10.1093/molbev/msae263

Lemoine F, Correia D, Lefort V, *et al.* (2019). NGPhylogeny.fr: new generation phylogenetic services for non-specialists. *Nucleic Acids Research* **47**: W260–W265. https://doi.org/10.1093/nar/gkz303

Leplat J, François A, Bousta F (2022a). Diversity of *Parengyodontium* spp. strains isolated from the cultural heritage environment: phylogenetic diversity, phenotypical diversity, and occurrence. *Mycologia* **114**: 1–16. https://doi.org/10.1080/00275514.2022.2094046

Leplat J, François A, Bousta F (2022b). *Leptobacillium cavernicola*, a newly discovered fungal species isolated from several Paleolithic-decorated caves in France. *Phytotaxa* **571**: 186–196. https://doi.org/10.11646/phytotaxa.571.2.5

Leplat J, François A, Bousta F (2020a). *Parengyodontium album*, a frequently reported fungal species in the cultural heritage environment. *Fungal Biology Reviews* **34**: 126–135. https://doi.org/10.1016/j.fbr.2020.06.002

Leplat J, Francois A, Bousta F (2017). White fungal covering on the wall paintings of the Saint-Savin-sur-Gartempe Abbey church crypt: a case study. *International Biodeterioration & Biodegradation* **122**: 29–37. https://doi.org/10.1016/j.ibiod.2017.04.007

Leplat J, François A, Touron S, *et al.* (2020b). Aerobiological behavior of Paleolithic rock art sites in Dordogne (France): a comparative study in protected sites ranging from rock shelters to caves, with and without public access. *Aerobiologia* **36**: 355–374. https://doi.org/10.1007/s10453-020-09637-9

Leplat J, François A, Touron S, *et al.* (2019). Aerobiological behavior of Paleolithic decorated caves: a comparative study of five caves in the Gard department (France). *Aerobiologia* **35**: 105–124. https://doi.org/10.1007/s10453-018-9546-2

Magyar D, Strażyński P, Grewling Ł, *et al.* (2023). The contribution of aphids (*Aphidoidea*) to atmospheric concentrations of *Alternaria* and *Cladosporium* spores. *Aerobiologia* **39**: 1–17. https://doi.org/10.1007/s10453-023-09797-4

Mammola S, Pavlek M, Huber BA, *et al.* (2022). A trait database and updated checklist for European subterranean spiders. *Scientific Data* **9**: 1–13. https://doi.org/10.1038/s41597-022-01316-3

Mammola S, Piano E, Giachino PM, *et al.* (2017). An ecological survey of the invertebrate community at the epigean/hypogean interface. *Subterranean Biology* **24**: 27. https://doi.org/10.3897/subtbiol.24.21585

Mantzoukas S, Lagogiannis I, Kitsiou F, *et al.* (2023). Entomopathogenic action of wild fungal strains against stored product beetle pests. *Insects* **14**: 91. https://doi.org/10.3390/insects14010091

Martin-Sanchez PM, Jurado V, Porca E, *et al.* (2014). Airborne microorganisms in Lascaux Cave (France). *International Journal of Speleology* **43**: 295–303. https://doi.org/10.5038/1827-806X.43.3.6

Mitova MM, Iliev M, Nováková A, *et al.* (2017). Diversity and biocide susceptibility of fungal assemblages dwelling in the Art Gallery of Magura Cave, Bulgaria. *International Journal of Speleology* **46**: 67–80. https://doi.org/10.5038/1827-806X

Moog O, Christian E, Eis R (2021). Increased cave use by butterflies and moths: a response to climate warming? *International Journal of Speleology* **50**: 15–24. https://doi.org/10.5038/1827-806X.50.1.2361

Mulec J, Vaupotič J, Walochnik J (2012). Prokaryotic and

eukaryotic airborne microorganisms as tracers of microclimatic changes in the underground (Postojna Cave, Slovenia). *Microbial Ecology* **64**: 654–667. https://doi.org/10.1007/s00248-012-0059-1

Nonaka K, Kaifuchi S, Ōmura S, *et al.* (2013). Five new *Simplicillium* species (*Cordycipitaceae*) from soils in Tokyo, Japan. *Mycoscience* **54**: 42–53. https://doi.org/10.1016/j.myc.2012.07.002

Nováková A (2009). Microscopic fungi isolated from the Domica Cave system (Slovak Karst National Park, Slovakia). A review. *International Journal of Speleology* **38**: 71–82. https://doi.org/10.5038/1827-806X.38.1.8

Novakova A, Hubka V, Valinová Š, *et al.* (2018). Cultivable microscopic fungi from an underground chemosynthesis-based ecosystem: a preliminary study. *Folia Microbiologica* **63**: 43–55. https://doi.org/10.1007/s12223-017-0527-6

Okane I, Nonaka K, Kurihara Y, *et al.* (2020). A new species of *Leptobacillim*, *L. symbioticum*, isolated from mites and sori of soybean rust. *Mycoscience* **61**: 165–171. https://doi.org/10.1016/j.myc.2020.04.006

Pangallo D, Chovanová K, Šimonovičová A, *et al.* (2009). Investigation of microbial community isolated from indoor artworks and air environment: identification, biodegradative abilities, and DNA typing. *Canadian Journal of Microbiology* **55**: 277–287. https://doi.org/10.1139/W08-136

Parker CW, Teixeira M de M, Singh NK, *et al.* (2022). Genomic characterization of *Parengyodontium torokii* sp. nov., a biofilm-forming fungus isolated from Mars 2020 assembly facility. *Journal of Fungi* **8**: 66. https://doi.org/10.3390/jof8010066

Pasquarella C, Balocco C, Pasquariello G, *et al.* (2015). A multidisciplinary approach to the study of cultural heritage environments: experience at the Palatina Library in Parma. *Science of the Total Environment* **536**: 557–567. https://doi.org/10.1016/j.scitotenv.2015.07.105

Pavlović J, Puškárová A, Planý M, *et al.* (2023). Colored stains: microbial survey of cellulose-based and lignin rich papers. *International Journal of Biological Macromolecules* 124456. https://doi.org/10.1016/j.ijbiomac.2023.124456

Perera RH, Hyde KD, Jones EBG, *et al.* (2023). Profile of *Bionectriaceae*, *Calcarisporiaceae*, *Hypocreaceae*, *Nectriaceae*, *Tilachlidiaceae*, *Ijuhyaceae* fam. nov., *Stromatonectriaceae fam. nov.* and *Xanthonectriaceae fam. nov. Fungal Diversity* **118**: 95–271. https://doi.org/10.1007/s13225-022-00512-1

Piel WH, Donoghue M, Sanderson M, *et al.* (2000). TreeBASE: a database of phylogenetic information. Presented at the Proceedings of the 2nd International Workshop of Species.

Pinheiro AC, Sequeira SO, Macedo MF (2019). Fungi in archives, libraries, and museums: a review on paper conservation and human health. *Critical Reviews in Microbiology* **45**: 686–700. https://doi.org/10.1080/1040841X.2019.1690420

Pinzari F (2011). Microbial ecology of indoor environments: the ecological and applied aspects of microbial contamination in archives, libraries and conservation environments. In: *Sick Building Syndrome: In Public Buildings and Workplaces* (Abdul-Wahab, SA ed.). Springer, New York, USA: 153–178.

Ponizovskaya VB, Grum-Grzhimaylo AA, Georgieva ML, *et al.* (2020). *Lecanicillium gracile* (*Cordycipitaceae*), a new species isolated from mineral building materials. *Phytotaxa* **443**: 265–278. https://doi.org/10.1016/S0964-8305(97)00062-0

Ramanujam B, Poornesha B, Kandan A, *et al.* (2021). Natural occurrence of entomopathogenic fungus *Beauveria felina* (DC.) JW Carmich on fall armyworm, *Spodoptera frugiperda* (JE Smith). *Journal of Entomology and Zoology Studies* **9**: 140–143. https://doi.org/10.22271/j.ento.2021.v9.i3b.8738

Rehner SA, Minnis AM, Sung GH, *et al.* (2011). Phylogeny and systematics of the anamorphic, entomopathogenic genus *Beauveria*. *Mycologia* **103**: 1055–1073. https://doi.org/10.3852/10-302

Ren Y, Wu C, Wang L, *et al.* (2023). Fading mechanism of the blue and green pigments on Chinese polychrome pottery of the Tang Dynasty: First discovery of *Simplicillium aogashimaense* strain on artifacts. *Journal of Cultural Heritage* **62**: 181–186. https://doi.org/10.1016/j.culher.2023.05.028

Roberts DW, Leger RJS (2004). *Metarhizium* spp., cosmopolitan insect-pathogenic fungi: Mycological aspects. *Advances in Applied Microbiology* **54**: 1–70. https://doi.org/10.1016/S0065-2164(04)54001-7

Rojas TI, Aira MJ, Batista A, *et al.* (2012). Fungal biodeterioration in historic buildings of Havana (Cuba). *Grana* **51**: 44–51. https://doi.org/10.1080/00173134.2011.643920

Ronquist F, Teslenko M, Van Der Mark P, *et al.* (2012). MrBayes 3.2: efficient Bayesian phylogenetic inference and model choice across a large model space. *Systematic Biology* **61**: 539–542. https://doi.org/10.1093/sysbio/sys029

Sanchez-Moral S, Jurado V, Fernandez-Cortes A, *et al.* (2021). Environment-driven control of fungi in subterranean ecosystems: the case of La Garma Cave (northern Spain). *International Microbiology* **24**: 1–19. https://doi.org/10.1007/s10123-021-00193-x

Santamaria S, Faille A (2007). *Rhachomyces (Ascomycota*, *Laboulbeniales*) parasites on cave-inhabiting Carabid beetles from the Pyrenees. *Nova Hedwigia* **85**: 159–186. https://doi.org/10.1127/0029-5035/2007/0085-0159

Scheerer S, Ortega-Morales O, Gaylarde C (2009). Microbial deterioration of stone monuments—an updated overview. *Advances in Applied Microbiology* **66**: 97–139. https://doi.org/10.1016/S0065-2164(08)00805-8

Spatafora JW, Sung GH, Sung JM, *et al.* (2007). Phylogenetic evidence for an animal pathogen origin of ergot and the grass endophytes. *Molecular Ecology* **16**: 1701–1711. https://doi.org/10.1111/j.1365-294X.2007.03225.x

Stamatakis A (2014). RAxML version 8: a tool for phylogenetic analysis and post-analysis of large phylogenies. *Bioinformatics* **30**: 1312–1313. https://doi.org/10.1093/bioinformatics/btu033

Sterflinger K (2010). Fungi: their role in deterioration of cultural heritage. *Fungal Biology Reviews* **24**: 47–55. https://doi.org/10.1016/j.fbr.2010.03.003

Sterflinger K, Pinzari F (2012). The revenge of time: fungal deterioration of cultural heritage with particular reference to books, paper and parchment. *Environmental*

Microbiology **14**: 559–566. https://doi.org/10.1111/j.1462-2920.2011.02584.x

Stupar M, Savković Ž, Popović S, *et al.* (2023). Speleomycology of air in Stopića cave (Serbia). *Molecular Ecology* **86**: 2021–2031. https://doi.org/10.1007/s00248-023-02214-w

Sukarno N, Kurihara Y, Park J-Y, *et al.* (2009). *Lecanicillium* and *Verticillium* species from Indonesia and Japan including three new species. *Mycoscience* **50**: 369–379. https://doi.org/10.1007/S10267-009-0493-1

Sun JZ, Liu XZ, Hyde KD, *et al.* (2017). *Calcarisporium xylariicola* sp. nov. and introduction of *Calcarisporiaceae* fam. nov. in *Hypocreales*. *Mycological Progress* **16**: 433–445. https://doi.org/10.1007/s11557-017-1290-4

Sung GH, Hywel-Jones NL, Sung JM, *et al.* (2007). Phylogenetic classification of *Cordyceps* and the clavicipitaceous fungi. *Studies in Mycology* **57**: 5–59. https://doi.org/10.3114/sim.2007.57.01

Talavera G, Castresana J (2007). Improvement of phylogenies after removing divergent and ambiguously aligned blocks from protein sequence alignments. *Systematic Biology* **56**: 564–577. https://doi.org/10.1080/10635150701472164

Teixeira MM, Muszewska A, Travis J, *et al.* (2020). Genomic characterization of *Parengyodontium americanum sp. nov*. *Fungal Genetics and Biology* **138**: 103351. https://doi.org/10.1016/j.fgb.2020.103351

Trovão J, Mesquita N, Paiva DS, *et al.* (2013). Can arthropods act as vectors of fungal dispersion in heritage collections? A case study on the archive of the University of Coimbra, Portugal. *International Biodeterioration & Biodegradation* **79**: 49–55. https://doi.org/10.1016/j.ibiod.2012.10.015

Trovão J, Portugal A, Soares F, *et al.* (2019). Fungal diversity and distribution across distinct biodeterioration phenomena in limestone walls of the old cathedral of Coimbra, UNESCO World Heritage Site. *International Biodeterioration & Biodegradation* **142**: 91–102. https://doi.org/10.1016/j.ibiod.2019.05.008

Vanderwolf KJ, Malloch D, McAlpine DF, *et al.* (2013). A world review of fungi, yeasts, and slime molds in caves. *International Journal of Speleology* **42**: 77–96. https://doi.org/10.5038/1827-806X.42.1.9

Vaughan MJ, Maier RM, Pryor BM (2011). Fungal communities on speleothem surfaces in Kartchner Caverns, Arizona, USA. *International Journal of Speleology* **40**: 65–77. https://doi.org/10.5038/1827-806X.40.1.8

Wang YB, Tang DX, Duan DE, *et al*. (2020a). Morphology, molecular characterization, and virulence of *Beauveria pseudobassiana* isolated from different hosts. *Journal of Invertebrate Pathology* **172**: 107333. https://doi.org/10.1016/j.jip.2020.107333

Wang YB, Wang Y, Fan Q, *et al*. (2020b). Multigene phylogeny of the family *Cordycipitaceae* (*Hypocreales*): new taxa and the new systematic position of the Chinese cordycipitoid fungus *Paecilomyces hepiali*. *Fungal Diversity* **103**: 1–46. https://doi.org/10.1007/s13225-020-00457-3

Weng Q, Zhang X, Chen W, *et al.* (2019). Secondary metabolites and the risks of *Isaria fumosorosea* and *Isaria farinosa*. *Molecules* **24**: 664. https://doi.org/10.3390/molecules24040664

Wynne JJ, Sommer S, Howarth FG, *et al.* (2018). Capturing arthropod diversity in complex cave systems. *Diversity and Distributions* **24**: 1478–1491. https://doi.org/10.1111/ddi.12772

Xiang CY, Gao F, Jakovlić I, *et al.* (2023). Using PhyloSuite for molecular phylogeny and tree-based analyses. *iMeta* **2**: e87. https://doi.org/10.1002/imt2.87

Yadav AN, Verma P, Kumar V, *et al.* (2018). Biodiversity of the genus *Penicillium* in different habitats. In: *New and Future Developments in Microbial Biotechnology and Bioengineering* (Gupta, Vijai Kumar, Rodriguez-Couto, S eds.). Elsevier, Amsterdam (The Netherlands): 3–18.

Yang J, Huang X, Tian B, *et al.* (2005). Characterization of an extracellular serine protease gene from the nematophagous fungus *Lecanicillium psalliotae*. *Biotechnology Letters* **27**: 1329–1334. https://doi.org/10.1007/s10529-005-0482-1

Yoder JA, Benoit JB, Christensen BS, *et al.* (2009). Entomopathogenic fungi carried by the cave orb weaver spider, *Meta ovalis* (*Araneae*, *Tetragnathidae*), with implications for mycoflora transfer to cave crickets. *Journal of Cave and Karst Studies* **71**: 116–120.

Yoder JA, Nelson B, Dobrotka C (2017). Water and temperature requirements for growth and possible role in infecting cave crickets by the entomopathogenic fungus *Beauveria caledonica* isolated from the cave beetle, *Darlingtonea kentuckensis* (*Coleoptera*: *Carabidae*). *Speleobiology Notes* **9**: 11–17.

Zare R, Gams W (2016). More white verticillium-like anamorphs with erect conidiophores. *Mycological Progress* **15**: 993–1030. https://doi.org/10.1007/s11557-016-1214-8

Zare R, Gams W (2001). A revision of *Verticillium* section *Prostrata*. IV. The genera *Lecanicillium* and *Simplicillium* gen. nov. *Nova Hedwigia* **73**: 1–50. https://doi.org/10.1127/nova.hedwigia/71/2001/1

Zhang W, Zhang X, Li K, *et al.* (2018). Introgression and gene family contraction drive the evolution of lifestyle and host shifts of hypocrealean fungi. *Mycology* **9**: 176–188. https://doi/org/10.1080/21501203.2018.1478333

Zhang ZF, Liu F, Zhou X, *et al.* (2017). Culturable mycobiota from karst caves in China, with descriptions of 20 new species. *Persoonia* **39**: 1–31. https://doi.org/10.3767/persoonia.2017.39.01

Zhang ZF, Zhou SY, Eurwilaichitr L, *et al.* (2020). Culturable mycobiota from karst caves in China II, with descriptions of 33 new species. *Fungal Diversity* **106**: 29–136. https://doi.org/10.1007/s13225-020-00453-7

Zhou YM, Zhi JR, Qu JJ, *et al.* (2022). Estimated divergence times of *Lecanicillium* in the family *Cordycipitaceae* provide insights into the attribution of *Lecanicillium*. *Frontiers in Microbiology* **13**: 1379. https://doi.org/10.3389/fmicb.2022.859886

Zhu M, Duan X, Cai P, *et al.* (2022). Deciphering the genome of *Simplicillium aogashimaense* to understand its mechanisms against the wheat powdery mildew fungus *Blumeria graminis* f. sp. *tritici*. *Phytopathology Research* **4**: 16. https://doi.org/10.1186/s42483-022-00121-5

Zimmermann G (2007). Review on safety of the entomopathogenic fungi *Beauveria bassiana* and *Beauveria brongniartii*. *Biocontrol Science and Technology* **17**: 553–596. https://doi.org/10.1080/09583150701309006

Zucconi L, Canini F, Isola D, *et al.* (2022). Fungi affecting wall paintings of historical value: A worldwide meta-analysis of their detected diversity. *Applied Sciences* **12**: 2988. https://doi.org/10.3390/app12062988

Supplementary Material: http://fuse-journal.org/

Table S1. Fungal taxa used in the phylogenetic study

Studied species are displayed in bold print. Newly described species from studied strains are displayed in bold red print.

Fig. S1. Phylogenetic studies through maximum likelihood (ML) and Bayesian inference (BI) of the studied strains at the order level. The trees were rooted with *Cephalotrichum gorgonifer* (*Microascales*; accession number ONZQ00000000) as an outgroup. The genera were collapsed by families when it was possible. Bootstrap values greater than or equal to 70 % and Bayesian posterior probabilities greater than or equal to 0.70 are located close to the corresponding nodes. The number of studied strains recovered in each family is displayed in brackets after the family name. Newly described genera and species from studied strains are displayed in bold red print.

Fig. S2. Phylogenetic studies through maximum likelihood (ML) and Bayesian inference (BI) in the *Bionectriaceae*. The trees were rooted with *Gamszarea wallacei* CBS 101237 (*Cordycipitaceae*) as an outgroup. Bootstrap values greater than or equal to 70 % and Bayesian posterior probabilities greater than or equal to 0.70 are located close to the corresponding nodes. The studied strains are displayed in bold print.

Fig. S3. Phylogenetic studies through maximum likelihood (ML) and Bayesian inference (BI) among *Amphichorda* species. The trees were rooted with *Stilbocrea walteri* CBS 144627 (*Bionectriaceae*) as an outgroup. Bootstrap values greater than or equal to 70 % and Bayesian posterior probabilities greater than or equal to 0.70 are located close to the corresponding nodes. The studied strain is displayed in bold print.

Figure S4. Phylogenetic studies through maximum likelihood (ML) and Bayesian inference (BI) in the *Cordycipitaceae*. The trees were rooted with *Amphichorda guana* CGMCC 3.17908 (*Bionectriaceae*) as an outgroup. Bootstrap values greater than or equal to 70 % and Bayesian posterior probabilities greater than or equal to 0.70 are located close to the corresponding nodes. The studied strains are displayed in bold print. Previously described species which need to be considered for a new combination are displayed in blue print.

Fig. S5. Phylogenetic studies through maximum likelihood (ML) and Bayesian inference (BI) among *Beauveria* species. The trees were rooted with *Gamszarea wallacei* CBS 101237 (*Cordycipitaceae*) as an outgroup. Bootstrap values greater than or equal to 70 % and Bayesian posterior probabilities greater than or equal to 0.70 are located close to the corresponding nodes. The studied strains are displayed in bold print.

Fig. S6. Phylogenetic studies through maximum likelihood (ML) and Bayesian inference (BI) among *Cordyceps* species. The trees were rooted with *Gamszarea wallacei* CBS 101237 (*Cordycipitaceae*) as an outgroup. Bootstrap values greater than or equal to 70 % and Bayesian posterior probabilities greater than or equal to 0.70 are located close to the corresponding nodes. The studied strains are displayed in bold print.

Fig. S7. Phylogenetic studies through maximum likelihood (ML) and Bayesian inference (BI) among *Leptobacillium* species. The trees were rooted with *Cordyceps tenuipes* ARSEF 5135 (*Cordycipitaceae*) as an outgroup. Bootstrap values greater than or equal to 70 % and Bayesian posterior probabilities greater than or equal to 0.70 are located close to the corresponding nodes. The studied strains are displayed in bold print.

Fig. S8. Phylogenetic studies through maximum likelihood (ML) and Bayesian inference (BI) among *Parengyodontium* species. The trees were rooted with *Cordyceps tenuipes* ARSEF 5135 (*Cordycipitaceae*) as an outgroup. Bootstrap values greater than or equal to 70 % and Bayesian posterior probabilities greater than or equal to 0.70 are located close to the corresponding nodes. The studied strains are displayed in bold print. The new combination of previously described species transferred outside *Parengyodontium* is displayed in blue print.

Fig. S9. Phylogenetic studies through maximum likelihood (ML) and Bayesian inference (BI) among *Samsoniella* species. The trees were rooted with *Cordyceps tenuipes* ARSEF 5135 (*Cordycipitaceae*) as an outgroup. Bootstrap values greater than or equal to 70 % and Bayesian posterior probabilities greater than or equal to 0.70 are located close to the corresponding nodes. The studied strains are displayed in bold print.

Figure S10. Phylogenetic studies through maximum likelihood (ML) and Bayesian inference (BI) in the *Clavicipitaceae*. The trees were rooted with *Amphichorda guana* CGMCC 3.17908 (*Bionectriaceae*) as an outgroup. Bootstrap values greater than or equal to 70 % and Bayesian posterior probabilities greater than or equal to 0.70 are located close to the corresponding nodes. The studied strains are displayed in bold print.

Fig. S11. Phylogenetic studies through maximum likelihood (ML) and Bayesian inference (BI) among *Metapochonia* species. The trees were rooted with *Torrubiella ratticaudata* ARSEF 1915 (*Clavicipitaceae*) as an outgroup. Bootstrap values greater than or equal to 70 % and Bayesian posterior probabilities greater than or equal to 0.70 are located close to the corresponding nodes. The studied strains are displayed in bold print.

Figure S12. Phylogenetic studies through maximum likelihood (ML) and Bayesian inference (BI) in the *Ophiocordycipitaceae*. The trees were rooted with *Amphichorda guana* CGMCC 3.17908 (*Bionectriaceae*) as an outgroup. Bootstrap values greater than or equal to 70 % and Bayesian posterior probabilities greater than or equal to 0.70 are located close to the corresponding nodes. The studied strains are displayed in bold print.

Fig. S13. Phylogenetic studies through maximum likelihood (ML) and Bayesian inference (BI) among *Purpureocillium* species. The trees were rooted with *Tolypocladium inflatum* OSC 71235 (*Ophiocordycipitaceae*) as an outgroup. Bootstrap values greater than or equal to 70 % and Bayesian posterior probabilities greater than or equal to 0.70 are located close to the corresponding nodes. The studied strain is displayed in bold print.